AMERICAN UNIVERSITY OF BEIRUT

COORDINATED MULTIPOINT IN HETEROGENEOUS
NETWORKS WITH OVERLAP WITHIN MICROCELL
EXPANDED REGIONS

by
JESSICA JAWAD KHORIATY

A thesis
submitted in partial fulfillment of the requirements
for the degree of Master of Engineering
to the Department of Electrical and Computer Engineering
of the Faculty of Engineering and Architecture
at the American University of Beirut

Beirut, Lebanon
April 2016

AMERICAN UNIVERSITY OF BEIRUT

COORDINATED MULTIPOINT IN HETEROGENEOUS
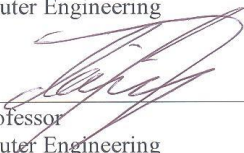NETWORKS WITH OVERLAP WITHIN MICROCELL
EXPANDED REGIONS

by
JESSICA JAWAD KHORIATY

Approved by:

_____   Advisor
Dr. Hassan Artail, Professor
Electrical and Computer Engineering

_____   Member of Committee
Dr. Zaher Dawy, Professor
Electrical and Computer Engineering

_____   Member of Committee
Dr. Youssef Nasser, Senior Lecturer
Electrical and Computer Engineering

Date of thesis defense: April 25, 2016

AMERICAN UNIVERSITY OF BEIRUT

THESIS, DISSERTATION, PROJECT RELEASE FORM

Student Name: _____
                         Last   First   Middle

◯ Master's Thesis   ◯ Master's Project   ◯ Doctoral Dissertation

☐   I authorize the American University of Beirut to: (a) reproduce hard or electronic copies of my thesis, dissertation, or project; (b) include such copies in the archives and digital repositories of the University; and (c) make freely available such copies to third parties for research or educational purposes.

☐   I authorize the American University of Beirut, **three years after the date of submitting my thesis, dissertation, or project,** to: (a) reproduce hard or electronic copies of it; (b) include such copies in the archives and digital repositories of the University; and (c) make freely available such copies to third parties for research or educational purposes.

_____

Signature   Date

ACKNOWLEDGMENTS

I would like to thank my advisor Prof. Hassan Artail for his continuous guidance throughout my Master's studies. I would also like to thank Prof. Zaher Dawy and Prof. Youssef Nasser for being part of the committee and for their helpful comments.

I would like to express my profound gratitude to my family. I thank my parents Jawad and Marlene Khoriaty for raising me with a love for knowledge and supporting me in all my endeavors. I am especially grateful to my aunt Rori for her continuous love, faith, and understanding. I would also like to thank my close friends for their encouragement throughout my studies.

Finally, I would like to thank Nouna, Pinky and Boggy. Without their help and support this thesis would not be possible.

AN ABSTRACT OF THE THESIS OF

Jessica Jawad Khoriaty   for   Master of Engineering
                                              Major: Electrical and Computer Engineering

Title: Coordinated Multipoint in Heterogeneous Networks with Overlap within Microcell Expanded Regions

The Third Generation Partnership Program's (3GPP) is developing further enhancements to Long Term Evolution Systems known as LTE Advanced (LTE-A). These modifications are aimed at fulfilling the requirements of a fourth generation (4G) technology mainly in terms of throughput and coverage. An improvement in throughput can be achieved by reducing the distance between the base station (BS) and user equipment (UE). Therefore, heterogeneous networks (HetNets) were introduced as a means to meet increasing traffic demands.

A HetNet is a multi-tier cellular network that consists of a macrocell tier overlaid with a microcell tier. Macrocell BSs typically have a higher power than microcell BSs. Furthermore, there is a need to offload traffic from the macrocell to the microcell. This can be achieved by expanding the region of the microcell so more users will be associated with it. This causes significant cross-tier interference. One method to improve coverage is to deploy coordinated multipoint (CoMP) within the microcell expanded region (ER). In CoMP, multiple BSs transmit the UE's data at the same time, mitigating interference and improving performance. Furthermore, a problem arises when considering microcells that are close to each other. In that case, there may be an overlap within the microcell ERs. Traditionally, CoMP would be performed by the serving microcell and macrocell. Within the overlapping region, however, significant interference would be seen from UEs associated with the nearby microcell. Therefore, it would make sense to have the microcell that shares an overlapping region to participate in CoMP with the macrocell and serving microcell. This approach should maximize gains by reducing interference.

Our proposed methodology considers the effect of overlapping microcell ERs and uses tools from stochastic geometry to analyze performance metrics in terms of outage probability. Another important consideration in our analysis is the effect on having non-ideal backhaul on the system. A non-ideal backhaul network implies having limited capacity and some latency. Coordinated multipoint increases the strain on the backhaul network since additional data, proportional to the number of cooperating base stations, needs to travel on backhaul links. Furthermore, delay should be minimal and less than one subframe duration in order for reported channel state information to

vi

remain valid. Therefore, capacity and delay need to be investigated in the context of a coordinated multipoint joint transmission. Our system considers the effect of having non-ideal backhaul in a cellular network with coordinated multipoint while taking into account overlaps in the microcell expanded region.

CONTENTS

ILLUSTRATIONS

CHAPTER I

INTRODUCTION

The migration from 3G to 4G systems, brought on by a need to satisfy improved performance requirements, was not achieved by LTE systems [1]. Performance targets for 4G systems consist of peak data rates of 1 Gbps in the downlink and 500 Mbps in the uplink. Between the years 2010 and 2015, mobile traffic was predicted to increase by about 30 times [2]. Furthermore, studies have demonstrated that decreasing the distance between the UE and its serving BS can bring significant performance improvements in terms of increasing capacity by a factor of 1600 [3]. The enhancements to LTE, under the umbrella of LTE-Advanced, necessitated the introduction of the concept of heterogeneous networks and coordinated multipoint to better serve increasing traffic demands and reduce the distance between BSs and UEs[2].

Heterogeneous cellular networks (HetNets) consist of a traditional macrocell tier overlaid with several small cell tiers. Small cell base stations operate at a lower power than macrocell base stations and serve to offload traffic from the macrocell network. In a homogeneous cellular network, cell association is based on maximum downlink received signal strength [4]. However, in the case of heterogeneous networks, this method hinders efficient traffic offloading from the macrocell network since the received signal strength from distant macrocell base stations may be stronger than that of closer small cell base stations. Another problem that arises in HetNets is due to the uplink transmission of the macrocell base stations to UEs that are in the neighborhood of microcells, thus creating interference at those microcells. This problem can be

remedied through applying a bias factor [7] at such UEs, which allows for the expansion of the small cell base station coverage area. This bias factor is a multiplicative term that serves to increase the received signal strength perceived at the UE, thus causing small cell handover to take place sooner.

As we just mentioned, the microcell downlink signal is weaker than that of the macrocell in the small cell expanded region (ER). The application of the bias factor results in an increase in the level of interference and noise in the ER, since the UE is not connected to the cell that provides the strongest signal. Inter cell interference coordination (ICIC) is therefore needed to provide better signal quality at the UEs in the ER.

Cooperation between BSs is one of the solutions for inter cell interference. In joint transmission CoMP, base stations cooperate with each other to transmit the same data to the UE. CoMP allows for the mitigation of inter cell interference and the increase of throughput for users at the cell edge [2]. Recent works, as shown in section II, benefit from CoMP by allowing cross tier coordination between macrocell and microcell users.

Our proposed scheme allows for cross tier coordination while taking into account overlaps in microcell expanded regions. In the case of overlap, two microcells and the nearest macrocell will use CoMP joint transmission as shown in Fig.1.
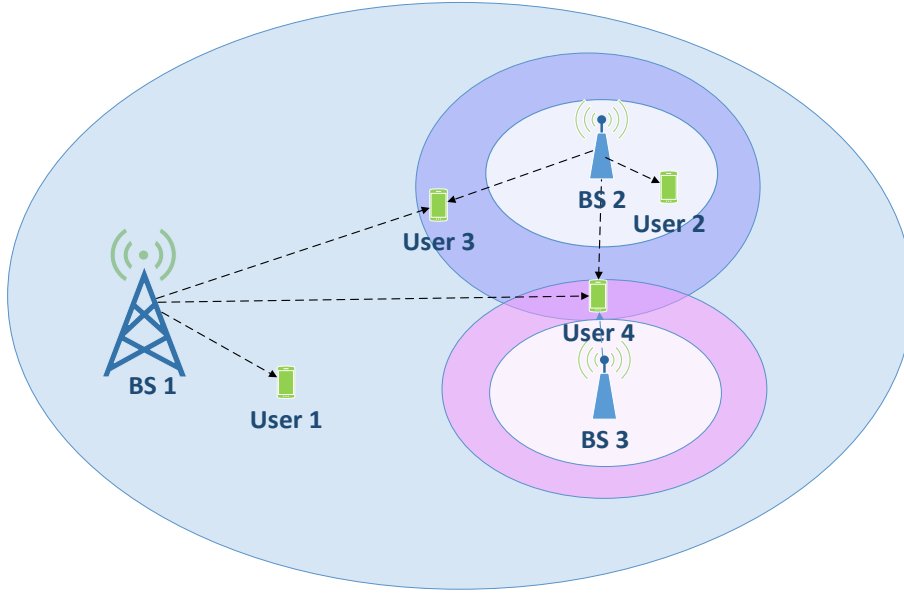
Figure 1: A two tier cellular network with one macrocell (BS1) and two microcells (BS2 and BS3). User 1 will be served by BS1, User 2 by BS2, user 3 by BS1 and BS2, and user 4 by BS1, BS2 and BS3.

Unlike previous work in the literature, our proposed method takes into account the effect of overlap in microcell expanded regions and serves to provide an analytical model for performance metrics such as outage probability. Outage probability is defined as the probability that the received SINR is lower than a certain threshold. This threshold can be used as an index to satisfy certain quality of service requirements.

In this proposal, we consider the expanded region around the microcell as the condition for employing CoMP joint transmission. In heavily crowded urban areas, the number of microcells could increase significantly in order to accommodate the rise in traffic demands. As the number of microcells increases, more micro BSs are likely to be located in close proximity to each other. This leads to regions that are likely to have densely located microcells with overlapping ERs. An overlap in the microcell ERs would have lower signal quality due to interference from two closely located BSs. In case of an overlap within two nearby microcell ERs, all three BSs will participate in CoMP. This approach would help to reduce interference by turning it into a useful

3

signal for each concerned UE. Beyond the ER, the ratio of the power between the macrocell base station and the strongest microcell base station is greater than a certain threshold. In that case, the user is served from a single macrocell base station since interference from the microcell would no longer be significant. Furthermore, the edges of the microcell coverage area consist of the region where the ratio of power between the macrocell base station and the microcell base station is 1. Therefore, within the microcell coverage area, the interference from the macrocell base station would no longer be significant and the users can be served solely by the microcell base station.

As discussed in [2], an important research challenge that needs to be addressed is the effect of having non-ideal backhaul on CoMP performance. Non-ideal backhaul consists of infrastructure with latency and capacity limitations. An important issue is the ability of a network to be able to support CoMP under non-ideal backhaul conditions. The quality that backhaul links must meet requires the handling of data exchange with low communication latency. This means that almost ideal backhaul links are needed for CoMP to be practical. This challenge is not addressed in [15]. In the literature, work was done focusing on reducing the CoMP backhaul burden by selecting a subset of base stations for cooperation. On the other hand, some work was aimed at investigating the effect of non-ideal backhaul in terms of delay incurred on the network. The importance of studying the effect of non-ideal backhaul lies in the fact that coordinated multipoint requires an increase in the amount of overhead traveling on the X2 interface. The overhead consists of the data that needs to be transmitted from the serving base station to the other base stations taking part in joint transmission CoMP. That way, multiple BSs can transmit the same data to a UE simultaneously. In terms of delay, the requirement is that the latency must be less than the duration of one subframe or 1ms.

4

This would ensure the validity of CSI against ageing channel conditions. Our proposed method is to study the effect of non-ideal backhaul in terms of capacity and delay limitations on our network scheme.

The content of this proposal consists of using tools from stochastic geometry to derive performance metrics related to location aware coordinated multipoint taking into account possible overlaps in microcell expanded regions. Furthermore, results in the literature are replicated and compared to the analytical model derived for expanded regions.

The main contributions of our work are as follows:

- Accounting for overlap regions that may result from deploying microcells close to each other.

- Using tools from stochastic geometry to derive performance metrics related to location aware coordinated multipoint transmission, taking into account possible overlaps in microcell expanded regions.

- Deriving the outage probability of the overall cellular network that also accounts for the overlaps in the microcell expanded regions, and comparing the results to those of similar systems found in the literature.

- Deriving the outage probability for users that lie within the microcell expanded region and comparing them to results of previous works in the literature.

- Providing a more scalable framework for CoMP, as compared to previous work, since overlaps in microcell expanded regions can occur in densely populated areas.

- Studying the effect of non-ideal backhaul on a CoMP system that takes into account overlaps within microcell expanded regions.

CHAPTER II

RELATED WORK

2.1. Long Term Evolution Advanced (LTE-A)

In the wake of the long term evolution of 3G services, the deployment of 4G services under the umbrella of LTE-Advanced come into play. A major leap in terms of quality of service and performance is required in LTE-A [3]. First of all, the downlink transmission mode in LTE as well as LTE-A is Orthogonal Frequency Division Multiplexing (OFDM). Data is being transmitted in multiple narrow bands which renders the complexity of equalization at the receiver end relatively low. In the downlink, however, power consumption becomes of a greater concern and therefore lowering the peak to average power ratio (PAPR) becomes more of a concern. This leads to the use of single carrier frequency division multiple access (SC-FDMA) for the uplink. When it concerns inter-cell interference coordination, a frequency reuse factor of 1 is employed and, theoretically, there is no interference between UEs operating within the same cell. Therefore, in the literature, work is mostly concerned with mitigating interference between users in different cells. As part of LTE-A, peak data rates of 1 Gbps in the downlink and 500 Mbps in the uplink [2] lead to a higher SINR requirement at the receiver than previous generation technologies. This necessitates the reduction of the distance between the UE and its serving base station by introducing the concept of heterogeneous networks.

2.2. Small Cells and Heterogeneous Networks

Heterogeneous networks, where macrocell BSs are overlaid with another tier of microcell BSs, provide a viable way for increasing SINR at the receiver by effectively

reducing the distance between the UE and its serving BS. Small cells, or microcells are usually found in locations where traffic demands are high and serve to offload traffic from the macrocell BS. They operate at a lower power than the macrocell BS. At the same time, this raises concerns about intercell interference since the microcell is located within the macrocell transmission range.

Another effective method to reduce the distance between the BS and UE is the use of relay nodes, also part of the LTE-A framework. The relay node serves as an intermediate step between the BS and the UE. It acts as both a UE and BS at the same time. When it acts as a UE or communicates with the BS, it is connected to the BS via the Un interface. When it acts as a BS or communicates with the UE, it is connected via the Uu interface [4]. There are different types of relay nodes. Amplify and forward (AF) or repeaters simply transmit the received signal by amplifying it to the UE. Decode and forward (DF) relays, perform processing such as error detection and correction, before forwarding to the concerned UE [4].

In light of the use of these techniques for improving HetNet performance, we are mostly concerned in maximizing the number of users offloaded from the macro BS. This results in the need for some intercell interference mitigation schemes as discussed in the next section.

2.3. Microcell Expanded Regions and Bias Factors

As a way for increasing the amount of traffic associated with microcells, bias factors were applied to allow UEs to connect to the microcell BS sooner than if relying on SINR. This is emphasized by the fact that the closer a microcell BS gets to the macrocell BS, the lower its effective range. This can sometimes mean that a UE could

be connected to a BS that is further away instead of a nearby microcell [7]. The bias factor causes the received power from the microcell to be perceived as greater than it actually is, allowing for handover to take place sooner. This multiplicative factor is added on the receiver end to change the perceived received power from the microcell. However, the fundamental drawback of employing this approach is the increase in the amount of interference that ER UEs experience due to the fact that they are associated with a BS with relatively lower power. This interference will need to be remedied with effective intercell interference mitigation techniques.

2.4. Interference Mitigation Schemes in HetNets

The need for intercell mitigation techniques arises from the use of microcell BSs within the transmission range of the macrocell. This need is also emphasized upon considering the ER technique discussed in the section above. Some current interference mitigation solutions depend on coordinating transmissions between base stations like the use of almost blank subframes [9] and spectrum resource partitioning [9]. Almost blank subframes consist of control channels that do not cause any data traffic. They consume low amounts of power and if macrocells allow for such a configuration, the microcell and the UE can communicate during silent periods from the macrocell. The configuration settings are communicated via the OAM of X2 interface [9]. Spectrum resource partitioning involve adapting the use of resources based on the channel conditions. This is done by having some resources that are reserved for use by the microcell. However, these schemes are disadvantageous since they cause macrocell throughput losses in both the frequency and time domain.

2.5. Outage Probability Modelling

Some of the major contributions involve the use of analytical models to derive certain performance metrics. In [10], base an analytical model for a K-tier heterogeneous network is derived and an expression for outage probability is obtained. Base station locations for each tier were modeled using a Poisson Point Process (PPP) with each tier having different parameters in terms of transmitted power, fading parameters and average number of users associated. On the other hand, [11] studies the SINR distribution in the HetNet downlink by means of the use of a homogeneous PPP as well. These models only considered the case in which each UE is served by a single BS and did not account for the case of coordinated multipoint transmission.

2.6. Coordinated Multipoint (CoMP)

CoMP provides several advantages which include mitigating user interfere at the cell edge, increasing throughput and raising average rates. There are two CoMP schemes to be considered. In coordinated scheduling or coordinated beamforming cooperation involves solely scheduling and control decisions with data only being transmitted from one base station. In joint transmission or joint processing CoMP, data is available at several cooperating base stations and is sent simultaneously to be decoded coherently at the receiver. This mitigates the effect of intercell interference and increases throughput.

CoMP can be realized through either a centralized or distributed architecture. In the centralized setup, control information and data is collected at a central unit which then makes decisions on clustering, precoding and power allocation. On the other hand, a distributed architecture requires CSI to be collected at the serving cell which then

forwards the required information to other base stations within the cooperating cluster.

A scenario depicting distributed CoMP can be seen in Fig.2 below:
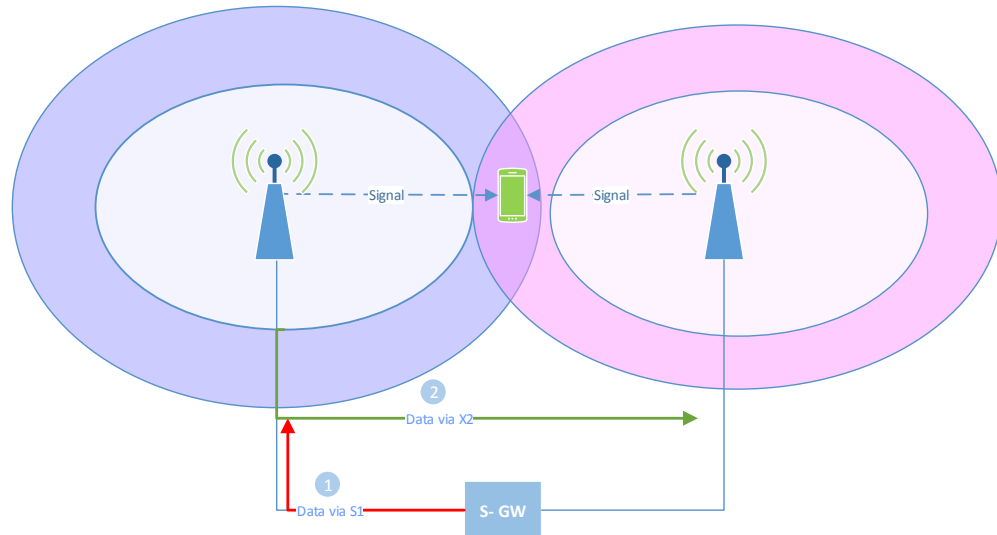
Figure 2: Two cells with overlapping expanded regions are cooperating via a distributed coordinated multipoint joint transmission scheme. The two base stations allocate the same time and frequency resources to the UE and transmit the same data in order to improve signal quality at the receiver. Each BS acts as a processing unit where precoded signals are computed.

The channel information that is required to be relayed back to the BSs in CoMP and as part of the CSI consists of the Channel Quality Indicator, Precoding Matrix Indicator, and Rank Indicator. This CSI is sent as feedback to the base stations which then cooperate in transmitting data simultaneously to the concerned UEs as seen in Fig.3.
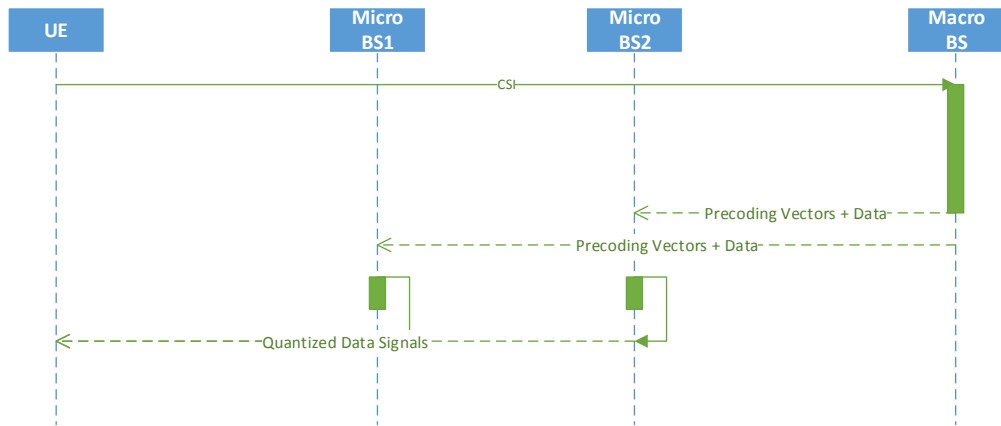
Figure 3: A UE sends CSI to the serving base station which then forwards the needed data to other BSs in the cooperating cluster.

Previous work on CoMP in HetNets mostly focuses on finding analytical models that represent the HetNet architecture which allows for the derivation of closed form expressions for certain performance metrics.   In [14], the authors provide a scheme for CoMP in a K-tier HetNet where the performance is analyzed in terms of outage probability. The base stations in each tier are distributed according to a spatial Poisson Point Process (PPP). An ideal backhaul network is assumed. However, this technique does not take into account the UE location, and therefore cannot be considered location aware. This causes analytical results to be different from those techniques that rely on location-based decisions for deploying CoMP.

2.7. Location Aware Coordinated Multipoint

A recent work that is described in [15] showed that using the bias factor technique alone for increasing to coverage area of a microcell is not sufficient and hence, they suggested a coordinated multipoint (CoMP) transmission framework between the macrocell base station and the small cell transmitter. In traditional CoMP, the backhaul network (i.e., X2 Interface) allows base stations to exchange control

information that allow them to cooperate in transmitting data to UEs [13] located at a point that is equidistant from three base stations, called a Voronoi vertex [14]. CoMP can be further extended to apply to heterogeneous networks [2].The advantage of using a CoMP framework between the small cell and macrocell is that it enhances signal quality without resource partitioning in frequency or time. That is, instead of having the macro base station signals act as interferers in the microcell vicinity, the macrocell base station can now actively cooperate in transmitting data along with the microcell.

The above work though has few limitations that need to be addressed. In fact, [15] implies that small cells are distant from each other and therefore the approach may not work efficiently in areas where small cells are heavily deployed. Therefore, we propose a system in which multiple small cell transmitters perform CoMP to strengthen the signal power in areas of overlap relative to the signal of the macrocell base station. The main contribution is to consider the effect of having CoMP between two microcells and one macrocell. We will also investigate the coordination of multiple small cell base stations with the macrocell base station to further improve signal quality in areas where several expanded regions overlap. Our proposed work adds a new level of cooperation between cells within the same tier and aims to solve interference problems in those overlapping regions. Hence, a scalable framework in terms of multiple small cell environments is provided.

2.8. Reducing Load on Backhaul in Coordinated Multipoint Systems

Backhaul literature consists of different categories. Some papers aim to reduce the backhaul load due to CoMP by selecting cooperating clusters instead of relying on full cooperation. The authors in [25] begin by claiming that theoretically, intercell

interference can be removed by having full network coordination between base stations. However, this is not feasible as it places a huge strain on the backhaul network. The paper aims to reduce the backhaul load by using a central coordinator to select a limited number of base stations for coordination.

The system model consists of a downlink channel with quality of service weights associated with each user. Base stations are grouped into clusters at each time slot. The paper states that there can be a number of methods to obtain the precoding matrix and assumes ZF precoding. An expression for the achievable rate and allocated power for a certain user is obtained. The paper considers a star network topology with a central unit (CU). Base stations send CSI estimates to the CU. Based on the CSI, the CU performs scheduling, clustering, beamforming calculation and power allocation and sends the information to the base stations. Base stations within the same cluster need to share user data among each other. Simulation results are shown for 19 base stations.

In [17], CoMP is applied only to a subset of users in order to obtain a compromise between the required performance improvements and the backhaul network constraints. The maximum achievable rate for each user is given as a function of a frequency flat channel matrix, transmit covariance and noise covariance. It is assumed that complete channel state information for each mobile is known at a central point in the network. It is also assumed that there are errorless but limited capacity links for the backhaul. In order to reduce the number of users that are employing CoMP and therefore reduce the amount of strain on the backhaul, the concept of groups is introduced. A group is defined as a set of users that are using the same resources across cells. The joint detection configuration gives the set of receive antennas and the number of quantization bits in which each user is detected, users in the same group are detected

by the same antennas with identical quantization bits. Then, the amount of backhaul that is needed to jointly serve users is calculated. This is the constraint that needs to be optimized. The paper then introduces the concept of isolation, which is proportional to how close the user is the cell center. Therefore, users are grouped according to isolation and those with weak isolation or close to the cell boundary are the ones that use CoMP. The number of users that are grouped depends on an algorithm that takes the backhaul capacity as a constraint. Furthermore, [18] improves on the previous paper by applying a system where a network is partitioned into subsystems and the algorithm can be applied to each subsystem. The system itself needs to have little knowledge of the whole system and CoMP is restricted to be within this subsystem. Knowledge of the local system is required and the assumption that all channel state information is present at a centralized point is not valid in a practical scenario and therefore no longer used. This results in having multiple decision making points based on local channel state information. Users cannot be served by a virtual MIMO operation across different subsystems except if the subsystems overlap and decision makers choose how to take care of common users. Another option can be to exchange information between subsystems. These two schemes cause strain on the backhaul due to the requirement of having communication between different decision makers. Therefore, the paper suggests defining subsystems according to a resource partitioning scheme where most interferers belong to the same subsystem and can be organized through MIMO. The grouping is done in the region where three cells meet which is where interference is greatest. The strongest interfering UEs are cancelled when they are assigned to the same resource block. This process continues for all the UEs in this region. The subsystem should cover 5 cells for interference mitigation to be significant. Furthermore, UEs that

are close to the BS have strong enough SINR to not need this interference mitigation scheme. This results in having each cell split into 5 areas and resources split into 5 equal blocks. Then for each subsystem the algorithm in the previous paper is run. The overhead needed is a notification on the backhaul capacity and a global scheduler that allows adjacent subsystems to take turns in the optimization. Also, [24] analyzes the mean packet delay and uses it to propose a BS association method based on range expansion. The analysis results in finding an optimal backhaul aware bias factor.

The system model consists of the components gateways, macro cell BS, small cell BS and users. MBSs and gateways are connected to the core via fiber links. SBSs are connected to the gateways via wireless links. The model assumes that the delay on the links from gateways and MBSs to the core network is negligible. Packet delay is due to wireless retransmissions and depends on transmission time and load.

An SIR expression is given. Transmission is slotted in time and successful transmissions occur when the SIR is above a certain threshold. Using the Shannon capacity formula, the number of bits that can be transmitted is defined. Furthermore, the mean packet delay is defined as the sum of the backhaul and RAN delays. The mean packet delay expression is given for the SBS and MBS and the mean number of time slots needed for successful transmission is obtained as well. Then, the BS association problem is presented and the paper develops an association scheme to minimize mean packet delay.

On the other hand [19], proposes to reduce load on backhaul links through the choice of CoMP scheme to be employed. The paper studies downlink coordinated multipoint between two base stations and two users based on different backhaul capacities. The paper proposes the use of adaptive coordination where the base stations

switch between joint transmission and coordinated beamforming based on channel conditions. It is assumed that both BSs have perfect CSI and that they are connected by error free but capacity limited links.

Three cooperation schemes are considered. The first assumes that the messages are available at both base stations and that both BSs carry out joint transmission and dirty paper coding (DPC) redundantly. The second method assumes that the messages are available at only one BS which performs DPC, quantizes and transmits the signal to the other BS via backhaul. The third and final method is a mix of the two previous ones where a message is available at both BSs while the other is available at only one BS. Each one is transmitted according to the schemes described earlier. Finally, the authors derive the achievable rates of the system and calculates the precoding vectors. Finally, achievable performance and required backhaul are given. Simulation results show that the use of adaptive cooperation schemes are most beneficial when available backhaul is moderate.

2.9. Effect of non-ideal Backhaul

Another set of works attempt to study the effect of having non ideal and unreliable backhaul on CoMP. The paper [20] considers the effect of varying backhaul topologies on the gains obtained from deploying CoMP. A set of different scenarios is used to study which base stations are suitable for CoMP joint transmission from the RAN perspective. Whether the CSI is needed to be exchanged between BSs for JT-CoMP depends on the transmission scheme used. For dynamic cells selection (DCS) and open-loop MIMO, only user data needs to be exchanged. Advanced schemes such as closed- loop MIMO and multi-user MIMO (MU-MIMO) need the exchange of CSI

along with the user data. This need results in stricter latency requirements for the CSI to remain valid for the duration of one subframe (1ms). On the other hand, the capacity requirements on the backhaul depend on the number of cooperating BSs since the amount of data transmitted and therefore, the capacity needed, is directly proportional to that number. The limitation of other work in the literature is the discussion of backhaul limitations in an abstract way not taking into account actual topologies and considering either a full mesh network or only having nearby BSs connected through the backhaul. This paper employs realistic backhaul topologies with a certain delay and limited capacity. In LTE-A, the serving BS receives data from the S-GW, and then transmits it to all the BSs participating in CoMP. Besides the user data, information about the downlink channels between the UE and every CoMP BS needs to be measured by the UE itself and reported back to the BSs. Then, the BSs would send the CSI to a distributed or centralized controller in order for the precoding matrices to be calculated and then sent back to the BSs along with the scheduling information. That way, CoMP can be performed successfully. The least overhead when transmitting data to participating UEs is to send raw user data and the precoding matrices so that the encoding would be performed at the BS itself. Backhaul requirements can be summarized as having enough capacity to transmit the extra amount of user data needed and low latency for the CSI to remain valid. As for the backhaul topology, employing a full mesh topology to reduce latency is too expensive. Instead, a more cost-effective solution is to use a tree topology. This causes an increase in delay since the path between BSs is longer and forwarding needs to be done. The system model employed in the paper's simulation is as follows. First, the BSs are distributed within a certain area and then links are added between them. For each UE, the desired set of cooperating BSs

17

is chosen. The topologies studied are both the mesh and tree. All links have identical properties. The latency is assumed to be (link length)*1.45/c. 1.45 is the refraction index of a single-mode fiber (SMF). The link capacity was chosen as a way to vary the overprovisioning. It is *flcap*dcoop*. Where *dcoop* is the average data rate generated by UEs served via CoMP while *flcap* is the normalized link capacity. The method of choosing the BSs that belong to the CoMP cluster is based on choosing a certain radius that controls the size of the cluster. The serving BS transmits the data to all other BSs participating in CoMP. In the simulation, every UE is considered one at a time and then it is decided whether CoMP is feasible. This decision is based on factors such as latency and capacity of the links between BSs. In order to simplify the simulation, signaling traffic is neglected since it is small compared to the user data. Data between the BSs is exchanged via the logical X2 interface. The simulation is run for both the tree and mesh topologies. In order to further enhance its studies, the paper also considers the effect of supporting different technologies on the feasibility of CoMP. The first assumption is the support of layer 2 switching which means that IP processing occurs only at the BSs reducing latency. The second assumption is that the backhaul network supports multicast when data is transmitted from the serving BS to other CoMP BSs. The paper also presents a method for backhaul network preclustering where CoMP clusters are chosen according to the backhaul conditions instead of just CSI. At the same time, [23] uses a three tier Poisson Tree model to study a hierarchical backhaul of a hyper dense heterogeneous network (HDH). The system model consists of four components which are traffic concentrators (TCs), macro base stations (MBSs), small cell base stations (SBSs) and mobile terminals (MTs). Each MT is associated with either a MBS or SBS and each BS is associated with a TC.

18

A bias factor is applied so that cell association is based on biased received power. An expression for the MT SINR is obtained. The paper assumes full frequency reuse and a random or Round Robin scheduling. Coverage probability, average rate per MT and average aggregate rate are obtained.

Fiber optic links connect the each BS to one TC based on distance. The analysis considers ideal and capacity limited links and it is performed for different SBS densities. Finally, [28] investigates the impact of unreliable backhaul on network cooperation. In a heterogeneous network scheme, the authors assign link failure probability to backhaul links for the cooperating groups. The system model assumes that each user collects CSI and sends it to its serving BS. A control unit (CU) obtains the CSI from different BSs and calculates the scheduling and precoding parameters. In joint transmission user data needs to be exchanged between BSs in the same cluster, however, coordinated scheduling does not require data exchange.

The authors assume the use of zero forcing precoding as the coherent transmission scheme. An SINR expression is obtained which is used to define the cluster sum rate. The paper considers single cell transmission without coordination as a baseline. The network core sends the data to be transmitted by the BS to the user. Unreliable backhaul may cause the BSs to decode the data incorrectly. Since there is no cooperation, unreliable backhaul only affects the data transmission to the user in the baseline case. In centralized coordination, each BS sends collected CSI to the CU to make decisions accordingly. LFPs are modeled as independent binary random variables as an erasing mask causing losses in backhaul information. In the semi-distributed architecture, CSI is shared between cooperating BSs. Then each UE calculates its own precoding weights and power allocation vectors. Finally, the probability of a BS to

19

refrain from transmitting due to unreliable backhaul is obtained. Analytical results show the effect of unreliable backhaul on performance. Coordinated scheduling is more resilient to unreliable backhaul. In joint transmission with more than two cooperating BSs, centralized coordination performs better than distributed coordination up to a certain limit.

2.10. Delay Model for Backhaul

Some papers aims to quantize delay in wireless backhaul due to the presence of heterogeneous networks. The results can be used to select an optimal density for small cell base stations. For instance, [21] employs a hierarchical model where each node connects to the closest node in the tier directly above it. The nodes are distributed according to a homogeneous Poisson Point Process. The paper seeks to obtain the expected downlink delay for a HetNet user. While the benefits of employing microcells may indicate that a user experiences lower delay when connected to the microcell base station, considering the effect of backhaul delay may show that this assumption may not always hold true.

The system model consists of a macrocell tier overlaid with a microcell tier. UEs are connected to a MBS or SAP wirelessly. The MBS are connected via fiber links to the core network aggregators (CNAs). At the same time, the SAPs are connected via wireless backhaul to the small cell gateways (SGs) which are linked to the CNAs via dedicated fiber. The paper considers two cases one for static or no mobility and another for high mobility and assumes negligible delay between the MBS and CNAs and the SGs and CNAs since they are connected via dedicated high capacity fiber. Another assumption is that the delay in the dedicated backhaul due to MBS is the same as the

delay due to SGs. Dedicated backhaul delay from the SGs and MBSs is not considered in the analysis.

Delay in wireless access is due to the need of retransmission in the case of failed reception. The model used in the paper is that a packet is transmitted repeatedly until it is successfully received up to a maximum of M times. A one bit ACK is sent upon successful reception or a one bit NACK would be sent. These messages have negligible delay and error. A successful transmission is when the SIR is above a certain threshold. At the same time, delay in wireless backhaul is the delay between the SAP and SG links. This is similar to the wireless access delay with a maximum number of retransmissions N. The paper assumes two wireless backhaul scenarios. These are in band and out of band wireless backhaul. In band wireless backhaul interferes with the SAP and MBS transmissions while the out of band backhaul does not.

An expression for the pdf of the length of a link between any two successive tiers is obtained. Then, the expected cost per link and the total expected cost are defined. Also, the average number of nodes connected to each node in the tier directly above is given. The deployment cost is also considered in the model. Base stations and users are denoted by their locations and an expression for SIR is obtained. Success probability is defined as the probability of having the SIR greater than a certain threshold. The probability of success is derived for a UE connected to a MBS and a UE connected to a SAP. These expressions are then used to derive the wireless delay for a typical user connected to a BS or SAP in the static and high mobility models which are both increasing functions in terms of transmitter x. A user connected to the nearest SAP instead of the nearest MBS will experience lower delay independent of mobility. This is due to the fact that the short distance to the SAP results in higher SIR. Then, the effect

of backhaul on delay is considered for out of band and in band backhaul. Expressions for outage probability are defined taking into account the limited number of allowed retransmissions.

The wireless backhaul delay decreases up to a limit as SAP density increases. This shows us that it would be useful to increase the SAP density up to a certain point. Then numerical results are obtained for varying SAP densities. The authors further extend this analysis in [22] where they present analysis and tradeoffs of having wired or wireless backhaul in a heterogeneous cellular network. Wired backhaul can be copper or fiber and has the advantage of increased reliability and capacity at a greater monetary cost to the operator. On the other hand, wireless backhaul is more cost effective and flexible but would have to account for interference with other devices operating on the same frequency bands. The choice of wireless or wired backhaul depends on the density of the microcells. The model builds on the one in paper 5 above. The network is modeled using a homogeneous Poisson Point Process for the nodes and the analysis is done for both static users and highly mobile users. The paper studies the average backhaul and network delays in a heterogeneous cellular network. The assumption of an ideal backhaul would indicate that users experience lower delay when connected to the microcells. However, having non-ideal backhaul shows that there may be cases where users experience lower delay when connected to the macrocell.

The system model consists of a macrocell tier overlaid with a microcell tier. UEs are connected to a MBS or SAP wirelessly. The MBS are connected via fiber links to the core network aggregators (CNAs). At the same time, the SAPs are connected via wired or wireless backhaul to the small cell gateways (SGs) which are linked to the CNAs via dedicated fiber. Each node is connected to the nearest node in the tier above

it. The paper considers the delay between the SAPs and the SGs. Other links have negligible delay. The authors begin by studying delay in wireless access which is due to retransmissions from packets that arrive in error. The packet would be transmitted until it is correctly received up to a maximum of M times. A successful transmission is when the SIR is above a certain threshold.

The paper presents the SINR expression and derives the probability of success for a wireless transmission from an SAP and MBS. These probabilities are then used to obtain the wireless access delay for a user connected to a MBS and a user connected to a SAP. The paper then shows that there is a lower delay when a user is connected to the nearest SAP compared to the nearest MBS. This is due to the fact that SAPs provide higher SINR due to the shorter distances. The delay in the wired backhaul is modeled as an exponentially distributed random variable. The mean is considered proportional to the average link distance and the average number of SAPs connected to the SGs. The wired backhaul delay is added to the expression for wireless access delay. Furthermore, the expected cost per link and the total expected cost are obtained. The paper also introduces a factor, beta, which represents how significant the backhaul delay is compared to the overall delay. In the case of wireless backhaul, the delay is obtained in a similar way to the wireless access delay. The paper considers two wireless backhaul scenarios. These are in band and out of band wireless backhaul. In band wireless backhaul interferes with the SAP and MBS transmissions while the out of band backhaul does not.

The paper also shows that increasing the number of SAPs beyond a certain point, increases the delay in accessing the small cell network. The paper then goes on to optimize delay from the network perspective. This is done by obtaining the association

23

probability to the SAP and MBS if association is distance based. Then the paper begins considering an interference based association policy and a delay based association policy and obtains the association probability in both cases. Finally the paper determines the optimal SAP densities to minimize delay for each association policy. Using wired backhaul allows for more reliability and allows for the computation of an ideal SAP density. Wireless backhaul, however, is less reliable but is more flexible in the choice of optimal SAP density. Finally, numerical results are shown.

2.11. Backhaul Traffic Estimation to Support CoMP

Several papers aim to provide schemes for network provisioning so that the backhaul would be able to support CoMP. The authors in [26] present a method to estimate the capacity needed for the backhaul network to support joint transmission coordinated multipoint. The amount of data exchanged between BSs depends on the size of the cooperating cluster. The paper discovers that 2/3 of the data exchange requires inter-site links for cluster sizes between 1 and 7. The paper relies on conclusion drawn by the next generation mobile network (NGMN) alliance that backhaul provisioning should account for 95 of the mobile traffic distribution since peak throughputs only occur in very lightly loaded cells. Coordinated multipoint increases peak cell throughput at the expense of increased backhaul traffic.

The LTE backhaul consists of two interfaces. S1 is a star network that connects cells to the advanced gateway. The X2 interface is a mesh that allows for traffic to travel between cells. Coordinated multipoint can be either centralized or distributed. Distributed joint transmission requires that the users transmit CSI to the serving cell which then transmits this information to all other BSs in the cluster. Then, precoding is

performed locally at each base station after data is exchanged between cells in the cluster. This method leads to a lower strain on the backhaul than in sending quantized signals to the BSs. The paper assumes that the traffic caused by exchanging CSI is negligible and that BSs and users have only one antenna.

For a certain cluster size S, the data exchanged on the X2 interface is (S-1) multiplied by a cell's own S1 traffic. This is correct if we assume similar traffic loads on nearby adjacent cells. The paper states that cluster size depends on whether the received signal strength from multiple base stations is within a certain window. Experimental results show that the maximum cluster size is 7, which corresponds to the hexagonal grid structure. The paper also claims that the backhaul traffic is increased only when cooperation is performed between inter-site cells. Then, based on spectral efficiency, system bandwidth and cluster size statistics, an estimate for S1 traffic is obtained. As a percentage of S1 traffic, expressions for X2 uplink and downlink traffic are obtained. The method in [26] is extended in [27] and aims to estimate traffic in a heterogeneous cellular network with cooperation. The paper assumes that small cells are connected in a hierarchical manner and that hosts serve as aggregation points (AGP) which transfer S1 traffic to the aGW. The paper also assumes that the network has knowledge of possible clusters and assigns those VLAN IDs.

For coordination, users measure the received signal strength within a certain window and send the list to the serving cell. The network then decides to form a cluster and uses cluster IDs to transmit data and CSI. Expressions similar to 10 above are obtained for uplink and downlink traffic based on instantaneous cluster size, however. The paper then obtains aggregate traffic for a three sectored macrocell site and then considers the feedback delay present. The delay for over the air transmission includes

25

the terminal processing delay and transmission delay due to packet size and data rate. The delay due to the exchange over the X2 interface includes the propagation and switching delay as well as the transmission delay. Finally, at the receiving BS, the decompression delay is incorporated into the analysis. Then, the authors investigate the SIR degradation due to the feedback delay and consider channel prediction to improve SIR.

Finally, [29] presents a more general approach where the paper analyzes the backhaul capacity requirements for coordinated multipoint based on channel characteristics and cluster size. The size of CSI is considered negligible. The architecture where BSs are connected to a radio network controller (RNC) which is connected to the internet is considered. The authors consider three cooperation modes. In the baseline mode, each BS serves one user and does its own processing. Data is sent to the BS from the RNC. The data rate is spectral efficiency multiplied by the channel bandwidth. In the limited coordination case, BSs transmit data only to their own users but scheduling information is shared so precoding matrices are designed to reduce interference between adjacent BSs. CSI may not need to be shared among different BSs in all cases. Under full coordination, data is shared among all BSs and transmitted to users simultaneously. This data can be sent as raw or quantized signals. This results in data rates similar to the baseline case but scaled with a factor equal to the cooperating cluster size.

2.12. Network Deployment Cost Analysis

A final consideration when looking into backhaul in communication networks would be the deployment cost. This is discussed in [30] where the paper aims to derive

the deployment cost of a three tier network, consisting of UEs, BSs and backhaul nodes, and to show that there exists a range of intensities for which costs are minimized while providing required user rates.

Each component in the network is modeled using a Poisson Point Process. Costs are classified into equipment, capacity and infrastructure costs. Equipment costs are incurred on the user. So to the service provider this is considered to be zero. Capacity cost is the cost of having links at a certain bandwidth and is proportional to distance. Infrastructure cost is the cost of making sure that two layers remain in connection. An analysis is done for fiber and wireless backhaul as well.

CHAPTER III

PROPOSED DESIGN

3.1. Two Tier Cellular Network Model

Our model consists of a macrocell tier overlaid with a microcell tier. The two tiers are independent. Each tier's BS position is modeled as a two dimensional homogeneous Poisson Point Process (PPP) with spatial intensity λ_1 for the macrocell and λ_2 for the microcell. Base stations belonging to the same tier are assumed to have the same transmit power and fading exponent. Furthermore, the users' positions are distributed according to homogeneous Poisson Point Process (PPP) with spatial intensity λ_u which is greater than λ_1 so that each base station will have at least one associated UE [15].
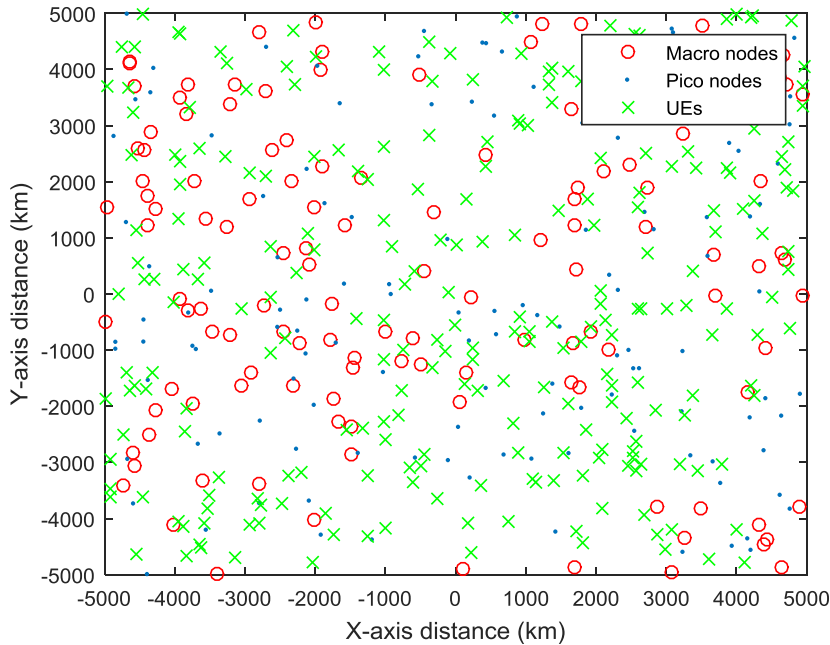
Figure 4: A Heterogeneous two tier cellular network with a macrocell tier overlaid with a microcell tier. Each tier is modeled as an independent Poisson Point Process. The UEs are also modeled using a Poisson Point Process with intensity higher than that of the microcell base stations to ensure that each BS has at least one UE to serve.

28

For illustration purposes, Fig.4 shows a hypothetical scenario illustrating the locations of different cellular network elements that consist of UEs, macro BSs, and micro BSs. The relation between the spatial intensities for each tier determines the relative number of each component in the network. For instance, if the ratio of λ_1 to λ_2 is 5, then for every macro base station, we would have 5 micro base stations on average.

3.2. Base station Association based on User Location

The choice of associated BS depends on the ratio of received powers from BSs in different tiers. In this work we consider four modes of operation: macrocell transmission only, microcell transmission only, CoMP between one macrocell and one microcell, and, finally, CoMP between one macrocell and two microcells. These can be abbreviated as the modes: M, P, 2C, 3C. In M mode, the user is associated with a macrocell BS when the ratio between the received power from the macrocell base station to the strongest received power from the microcell base station is greater than β. This means that the interference due to the microcell base station is low and coordination would not be necessary. In P mode, the user is associated with a microcell when the ratio between the received power from the macrocell base station to the strongest received power from the microcell base station is less than 1. This signifies that the cross tier interference in this zone is low and that cooperation is not necessary as well. 2C mode occurs within the microcell expanded region where the power ratio between the macrocell base station and the strongest microcell base station in between 1 and β. In this mode, the UE is served by one macro BS and one micro BS since the cross-tier interference is significant within this region. 3C mode occurs when there is an overlap in the expanded regions of the microcell with the strongest signal relative to the

29

UE and the microcell with the second strongest signal relative to the UE. The use of 3C mode in addition to 2C mode is the main contribution within this chapter. The cooperation of the second microcell is rendered necessary due to the fact that it would cause co-tier interference within the ER.

3.3. Base station Association

B is defined as the set of base stations that serve a particular user. The following equation denotes the possible base station association to a particular user:

$$
B = \begin{cases}
\{x_1\}, if\ \dfrac{P_1 R_1^{-\alpha_1}}{P_2 R_2^{-\alpha_2}} \geq \beta \\[3mm]
\{x_2\}, if\ \dfrac{P_1 R_1^{-\alpha_1}}{P_2 R_2^{-\alpha_2}} \leq 1 \\[3mm]
\{x_1, x_2\}, if\ 1 < \dfrac{P_1 R_1^{-\alpha_1}}{P_2 R_2^{-\alpha_2}} < \beta \wedge \overline{1 < \dfrac{P_1 R_1^{-\alpha_1}}{P_3 R_3^{-\alpha_3}} < \beta'} \\[3mm]
\{x_1, x_2, x_3\}, if\ 1 < \dfrac{P_1 R_1^{-\alpha_1}}{P_2 R_2^{-\alpha_2}} < \beta \wedge 1 < \dfrac{P_1 R_1^{-\alpha_1}}{P_3 R_3^{-\alpha_3}} < \beta'
\end{cases}
\tag{1}
$$

Where x_1 is a BS belonging to the macrocell tier and x_2 and x_3 are BSs belonging to the microcell tier. R_i ($i \in \{1,2,3\}$) is the distance from a typical user to the corresponding BS. As can be seen, we have three base stations of interest, one macrocell and two microcells. The threshold β represents the ratio of the power received from the macrocell BS to the strongest microcell BS while β' represents the ratio between the power received from the macrocell BS and the second strongest microcell BS. It follows that the values of β and β' determine the limits of the microcell expanded region. For the user to be in x_1 and associated with the microcell tier, the ratio of power received from the strongest macrocell to the power received from the strongest microcell should be greater that the threshold β. This means that the macrocell BS has the highest signal

30

strength and the user should be associated with it. In order for the user to be in x_2 region

and associated solely with a microcell, the ratio of the power between the strongest

macrocell and the strongest microcell should be less than 1. This means that the

microcell has the strongest signal and the user should be associated only with it. For the

user to be in the region of x_1 and x_2 or in association with one macrocell and one

microcell, the power ratio received from the strongest macrocell to the strongest

microcell should lie between 1 and β. This can be explained as being in the disk that we

have previously referred to as the microcell expanded region. Also, the ratio of the

power between the strongest macrocell and the second strongest microcell should not be

between 1 and β'. This means that we are outside the expanded region of the second

microcell of interest. Finally, for the user to be in the region x_1, x_2, and x_3 or the overlap

within the microcell expanded region, the ratio of power between the strongest

macrocell and the strongest microcell base stations should be between 1 and β. At the

same time, the power ratio between the strongest macrocell and the second strongest

macrocell base station should be within 1 and β'. This means that the user is located

within two expanded regions simultaneously and can benefit from having cooperation

from the three base stations of interest. This is the main contribution of our work in this

paper.

   The value of β and β' must be chosen as a tradeoff between performance gains

and increased backhaul signaling. This is due to the fact that higher values mean an

increase in the amount of coordination being performed in the network as a whole.

However, this increased level of coordination would cause more strain on the backhaul

network connecting the base stations. An important issue is the ability of a cellular

network to be able to support CoMP under non-ideal backhaul conditions. The quality

that backhaul links must meet requires the handling of data exchange with low communication latency. This challenge is not addressed in [15].

Again, referring to Fig.1, we can see that the received power by User 4 is within the ER of both BS2 and BS3, therefore the transmission mode 3C is used where the three BSs cooperate in transmitting the signal to User 4 instead of having only two cooperating base stations. Also, User 3 is served by BS1 and BS2 since it is in close proximity to BS2 and there is no overlap with the ER of BS3.

3.4. Distance Analysis

The probability that a user is in each one of the modes: *M*, *P*, *2C*, and *3C* is denoted by: q_M, q_P, q_{2C}, and q_{3C}, respectively. Based on these probabilities, the probability density functions (PDFs) of the distances between a UE and its serving BS are derived. Moreover, the probability of being in each of the four possible regions, as defined in (1) must be obtained. This is done within this section.

Based on the analysis done in [15], q_M and q_P can be obtained as follows:

$$q_M = 2\pi\lambda_1 \int_{R+} r \exp[-\pi(\lambda_1 r^2 + \lambda_2 \left(\frac{\beta P_2}{P_1}\right)^{2/\alpha_2} r^{2\alpha_1/\alpha_2})]dr \qquad (2)$$

$$q_P = 2\pi\lambda_2 \int_{R+} r \exp[-\pi(\lambda_2 r^2 + \lambda_1 \left(\frac{\beta P_1}{P_2}\right)^{2/\alpha_1} r^{2\alpha_2/\alpha_1})]dr \qquad (3)$$

The probability q_{3C} can be derived by considering that the UE is associated with three BSs in case the user is within the ER of the two microcell BSs. Therefore, the probability of the UE being located within the ER of the microcell with the second strongest received power must also be obtained. This probability is equivalent to the probability of having the power ratio between the macrocell BS and the second

32

strongest microcell BS less than β'. This means that the second microcell BS of interest can be used for CoMP as well.

$$q_{3C} = (1 - q_M - q_P) P\left(\frac{P_1 R_1^{-\alpha_1}}{P_3 R_3^{-\alpha_3}} < \beta' \right) \tag{4}$$

$$q_{2C} = (1 - q_M - q_P) P\left(\frac{P_1 R_1^{-\alpha_1}}{P_2 R_3^{-\alpha_2}} < \beta' \right) \tag{5}$$

Equation (4) is resolved into (5) since the second microcell BS belongs to tier 2 with a transmission power equal to the microcell transmission power, and the pathloss exponent is equal to the microcell tier pathloss exponent. The probability of being in the expanded region of the microcell with the second strongest received power can be seen in (6):

$$P\left(\frac{P_1 R_1^{-\alpha_1}}{P_2 R_3^{-\alpha_2}} < \beta \right) = 2\pi\lambda_2 \int_{R+} r \exp[-\pi(\lambda_2 r^2 + \lambda_2 (\beta')^{2/\alpha_2} r^2)] dr \tag{6}$$

Furthermore, in case the user in is not in the modes: q_M, q_P, or q_{3C}, we can infer that the user is in q_{2C}, mode:

The outage probability was computed using two methods, the first involves computing the integral expression in (9) and the second involves an approximation. This analysis is based on the fact that since the transmission range of the BSs is considered as circular, the intersection of the microcell base stations that are close to each other can be considered as an ellipse. The area of intersection between the two BSs can be computed as:

$$A = \beta^2 \arccos\left(\frac{d^2 + \beta^2 - \beta'^2}{2d\beta} \right) + \beta'^2 \arccos\left(\frac{d^2 + \beta'^2 - \beta^2}{2d\beta'} \right)$$

$$-\frac{1}{2}\sqrt{(-d+\beta+\beta')(d-\beta+\beta')(d+\beta+\beta')} \tag{7}$$

Where d is the average distance between the two closest microcells. In our analysis d is maximum at the value of $1+\beta$ and minimum at the value of 2β. The limits are obtained based on how close two microcell BSs have to be to each other in order to be able to cooperate. The average of these two distances results in the following value for d:

$$d = 0.5 + 1.5\beta \tag{8}$$

Finally, the value of A was divided by the area of the whole expanded region disk in order to obtain a fraction that represents the portion of the disk that contains an overlap.

Furthermore, in case the user in is not in the modes: q_M, q_P, or q_{3C}, we can infer that it is in the q_{2C} mode:

$$q_{2C} = 1 - q_M - q_P - q_{3C} \tag{9}$$

Next, the PDFs of the distances between a UE and its serving BS is obtained based on [15]:

$$f_{R_M}(r) = \frac{2\pi\lambda_1}{q_M} r \exp[-\pi(\lambda_1 r^2 + \lambda_2 \left(\frac{\beta P_2}{P_1}\right)^{2/\alpha_2} r^{2\alpha_1/\alpha_2})] \tag{10}$$

$$f_{R_P}(r) = \frac{2\pi\lambda_2}{q_P} r \exp[-\pi(\lambda_2 r^2 + \lambda_1 \left(\frac{P_1}{P_2}\right)^{2/\alpha_1} r^{2\alpha_2/\alpha_1})] \tag{11}$$

In order to obtain the PDF of the mode $3C$, we need to consider the probability that there are no base stations in a disk of radius r. This probability is given by:

$$\exp[-\pi\lambda r^2]$$

<div align="right">(12)</div>

This can be used to derive the PDF of *3C* mode:

$$f_R'(r) = \frac{d}{dr}(1 - \exp[\pi\lambda r^2])$$

<div align="right">(13)</div>

$$f_{R_{3C}}(r) = \frac{8\pi^3\lambda_1\lambda_2^2}{q_{3C}}r_1 r_2 r_3 \exp[-\pi(\lambda_2(r_2^2 + r_3^2) + \lambda_1 r_1^2)]$$

<div align="right">(14)</div>

Similarly, the PDF of the mode *2C* can be obtained as:

$$f_{R_{2C}}(r) = \frac{4\pi^2\lambda_1\lambda_2}{q_{2C}}r_1 r_2 \exp[-\pi(\lambda_2 r_2^2 + \lambda_1 r_1^2)]$$

<div align="right">(15)</div>

The PDF expressions are needed so we can obtain the expressions for the outage probabilities in the next section.

3.5. Outage Probability Analysis

In this section an expression for the outage probability is obtained based on certain SINR analysis.

The received signal power can be expressed as:

$$\sum_{x_i \in B}\frac{\sqrt{P}h_x}{\|x_i\|^{\frac{\alpha}{2}}}X + \sum_{x_i \in B^C}\frac{\sqrt{P}g_y}{\|x_i\|^{\frac{\alpha}{2}}}Y + Z$$

<div align="right">(16)</div>

Where the first sum represents the useful signal, while the second sum represents the interference signal. The term B^C denotes the complement of the set B, and represents the base stations that are interferers at the UE and which are not participating in the transmission to the concerned UE. The terms h_x and h_y are the small scale fading

coefficients that are assumed to be Rayleigh distributed leading to a power distribution with exponential amplitude and uniform phase. The variable α is the pathloss exponent, while X and Y are random variables that represent the data sequences that are transmitted from the serving and interfering BSs. Finally, Z is the Additive white Gaussian noise (AWGN), and we assume a channel with no CSI at the receiver.

The outage probability is the probability that the received signal to interference and noise ratio (SINR) is lower than a certain threshold θ. The equation shows the definition of outage probability for different modes of operation i.

$$O_i = 1 - \int_A P[SINR(B) > \tau] f_{R_i}(r) dr \tag{17}$$

For the different modes of operation, we have outage probabilities defined as O_M, O_P, O_{2C}, and O_{3C}, respectively. For instance, the outage probability O_M can be defined as the probability that the SINR at a UE operating in the M mode is lower than θ. The outage probability can be derived for each mode as:

$$O_M = 1 - \int_A P\left[\frac{\left|\sqrt{P_1} h_1 \|x_1\|^{\frac{-\alpha_1}{2}}\right|^2}{\sum_{x_i \neq x_1} P_i |g_i|^2 \|x_i\|^{-\alpha_i} + Z} > \tau\right] f_{R_M}(r) dr \tag{18}$$

$$O_P = 1 - \int_A P\left[\frac{\left|\sqrt{P_2} h_2 \|x_2\|^{\frac{-\alpha_2}{2}}\right|^2}{\sum_{x_i \neq x_2} P_i |g_i|^2 \|x_i\|^{-\alpha_i} + Z} > \tau\right] f_{R_P}(r) dr \tag{19}$$

$$O_{3C} = 1 - \int_A P\left[\frac{\left\| \left| \sqrt{P_1} h_1 \|x_1\|^{\frac{-\alpha_1}{2}} \right|^2 + \left| \sqrt{P_2} h_2 \|x_2\|^{\frac{-\alpha_2}{2}} \right| + \left| \sqrt{P_2} h_3 \|x_3\|^{\frac{-\alpha_2}{2}} \right|^2 \right\|}{\sum\limits_{x_i \neq x_1, x_2, x_3} P_i |g_i|^2 \|x_i\|^{-\alpha_i} + Z} > \tau \right] f_{R_{3C}}(r) dr \qquad (20)$$

$$O_{3C} = 1 - \int_A P\left[\frac{\left\| \left| \sqrt{P_1} h_1 \|x_1\|^{\frac{-\alpha_1}{2}} \right|^2 + \left| \sqrt{P_2} h_2 \|x_2\|^{\frac{-\alpha_2}{2}} \right|^2 \right\|}{\sum\limits_{x_i \neq x_1, x_2} P_i |g_i|^2 \|x_i\|^{-\alpha_i} + Z} > \tau \right] f_{R_{2C}}(r) dr \qquad (21)$$

Since the different operation modes are mutually exclusive, then the overall outage probability can be defined as:

$$O = q_M O_M + q_P O_p + q_{2C} O_{2C} + q_{3C} O_{3C} \qquad (22)$$

The outage probabilities for users in each mode can be defined as:

$$O_M = 1 - \int_{R+} \exp\left[\frac{-\theta \sigma_z^2}{P_1 r^{-\alpha_1}} \right] \prod_{j=1}^{2} L_{I_j}\left(\frac{\theta r^{\alpha_1}}{P_1} \right) f_{R_M}(r) dr \qquad (23)$$

$$O_P = 1 - \int_{R+} \exp\left[\frac{-\theta \sigma_z^2}{P_2 r^{-\alpha_2}} \right] \prod_{j=1}^{2} L_{I_j}\left(\frac{\theta r^{\alpha_2}}{P_2} \right) f_{R_P}(r) dr \qquad (24)$$

$$O_{3C} = 1 - \int_{3C} \exp\left[\frac{-\theta \sigma_z^2}{P_1 r_1^{-\alpha_1} + P_2 r_2^{-\alpha_2} + P_2 r_3^{-\alpha_2}} \right] \prod_{j=1}^{2} L^*_{I_j}\left(\frac{\theta}{P_1 r_1^{-\alpha_1} + P_2 r_2^{-\alpha_2} + P_2 r_3^{-\alpha_2}} \right) f_{R_{3C}}(r) dr \qquad (25)$$

$$O_{2C} = 1 - \int_{2C} \exp\left[\frac{-\theta \sigma_z^2}{P_1 r_1^{-\alpha_1} + P_2 r_2^{-\alpha_2}} \right] \prod_{j=1}^{2} L^*_{I_j}\left(\frac{\theta}{P_1 r_1^{-\alpha_1} + P_2 r_2^{-\alpha_2}} \right) f_{R_{2C}}(r) dr \qquad (26)$$

Where σ_z is the variance of the AWGN and $L^*_{I_j}$, L_{I_j} are defined as in [15]:

$$L_{I_j}\left(\frac{\theta r^{\alpha_i}}{P_i}\right) = \exp\left[-2\pi\lambda_j\left(\theta\frac{P_j}{P_i}\right)^{\frac{2}{\alpha_j}} r^{\frac{2\alpha_i}{\alpha_j}} F\left(\left(\frac{\alpha_{ij}}{\theta}\right)^{\frac{1}{\alpha_j}},\alpha_j\right)\right] \tag{27}$$

$$L_{I_j}^{\ *}(s) = \exp\left[-2\pi\lambda_j\left(sP_j\right)^{\frac{2}{\alpha_j}} F\left(\left(\frac{1}{sP_j}\right)^{\frac{1}{\alpha_j}} r_j,\alpha_j\right)\right] \tag{28}$$

Where α_{ij} is equal to β when $i=1$ and $j=2$ and is equal to 1 otherwise.

$F(y,\alpha)$ is defined as:

$$F(y,\alpha) = \int_y^\infty \frac{u}{1+u^\alpha}\,du \tag{29}$$

Obtaining the value of O_{2C} involves integrating the expression in (22) over the region 2C which is defined by the limits of the following two variables:

$$r_1 \geq 0 \tag{30}$$

$$\left(\frac{P_2}{P_1}\right)^{\frac{1}{\alpha_2}} r_1^{\frac{\alpha_1}{\alpha_2}} < r_2 < \left(\frac{\beta P_2}{P_1}\right)^{\frac{1}{\alpha_2}} r_2^{\frac{\alpha_1}{\alpha_2}} \tag{31}$$

The limits of r_2, which is the distance between the UE and the strongest transmitting microcell, are obtained from the disk conditions that we have resulting from the microcell expanded region.

Furthermore, obtaining the value of O_{3C} involves integrating the expression in (20) over the region 3C which is defined by the limits of the following three variables:

$$r_1 \geq 0 \tag{32}$$

$$\left(\frac{P_2}{P_1}\right)^{\frac{1}{\alpha_2}} r_1^{\frac{\alpha_1}{\alpha_2}} < r_2 < \left(\frac{\beta P_2}{P_1}\right)^{\frac{1}{\alpha_2}} r_2^{\frac{\alpha_1}{\alpha_2}} \qquad (33)$$

$$\left(\frac{\beta P_2}{P_1}\right)^{\frac{1}{\alpha_2}} r_1^{\frac{\alpha_1}{\alpha_2}} < r_3 < \beta'^{\frac{1}{\alpha_2}} r_2 \qquad (34)$$

As can be seen in the limits above, r_2 is limited to be within the microcell

expanded region. The limits of r_3, the distance between the UE and the second microcell

BS, are based on the fact that the maximum power ratio between the strongest microcell

base station and the second strongest microcell base station is at most β'. Also the

minimum value that r_3 can have is based on the power ratio in relation to the macrocell

BS. This value cannot be higher than β.

Another method was also used to compute the outage probability for O_{3C}. This

involves an approximation which related the outage probability within the overlap

region, to the outage probability within the two microcells closest to the UE. In this

method, the O_{3C} expression was integrated over the whole two expanded region disks

around the two strongest transmitting microcells to the UE. Then, the fraction which is

the ratio of the area of the intersecting region to the area of the entire two disks is used

to obtain the outage probability for the overlap region. The average distance between

the two BSs is assumed as shown in (8). Next, simulation and numerical results are

provided to further analyze the consequences of our implementation.

CHAPTER IV

OUTCOMES AND SIGNIFICANCE

We aim to accomplish several outcomes in relation to the implementation of the proposed system. The first is to replicate the analytical results presented in [15] in order to properly assess the performance gains obtained from considering the effect of deploying CoMP within the microcell ER. The second, would be to derive the appropriate equations that take into account the modifications necessitated by the proposed design. The third, would be to obtain analytical results for our proposed scheme and compare them to the results in [15]. The fourth outcome would be to perform simulations to verify the validity of the analytical results. The fifth and final outcome would be to study the effect of non-ideal backhaul on the proposed system.

Our work aims to apply the principles of stochastic geometry to heterogeneous cellular networks, and specifically to scenarios that involve the use of CoMP. It will therefore examine the overall gains obtained from using CoMP in the small cell ERs and contribute towards improving overall gains within the umbrella of LTE Advanced. That is, our work will contribute toward the realization of an effective means of improving coverage within HetNets that will bring us closer towards the realization the 3GPP requirements for 4G and LTE-A.

To verify the reliability of the system and test its performance, we will develop a mathematical model that provides a theoretical account of the behavior and performance of the system that will be evaluated according to the performance metric of

outage probability. Additionally, simulations will be used to validate the mathematical model and generate results that will be used to primarily evaluate and validate the analytical model. Further analysis could be also done based on the simulation results. A simulator that can be used to accomplish this task would be MATLAB which can be used to fulfill our required objectives.

MATLAB is a high level language that allows for powerful analysis of numerical computations and visualizations [16].

In MATLAB, a Poisson Point Process can be defined in order to perform Monte Carlo simulations related to the outage probability metrics of our proposed method.

Furthermore, the Mathematics Toolbox provides the means for evaluating the analytical results obtained in [15] and in our work.

CHAPTER V

RESULTS

5.1. MATLAB Code Implementation

In order to obtain results from the analytical models discussed above, results needed to be generated on MATLAB. All functions were developed based on the equations (1)-(29). A diagram of the MATLAB block components can be seen below in fig. 2. The main function contains the parameters for beta which is the strongest microcell expanded region in dB, beta prime which is the second strongest microcell expanded region in dB, lambda 1 which is the spatial intensity for the macrocell base station locations, lambda 2 which is the spatial intensity for the microcell base station locations, alpha 1 which is the Rayleigh channel fading coefficient for the macrocell base station transmission, alpha 2 which is the Rayleigh channel fading coefficient for the microcell base station transmission, P1 which is the transmission power of the macrocell base station in dBm, P2 which is the transmission power of the microcell base station in dBm, tau which is the outage probability threshold in dB, and sigmaz which is the variance of the Average White Gaussian Noise at the receiver.
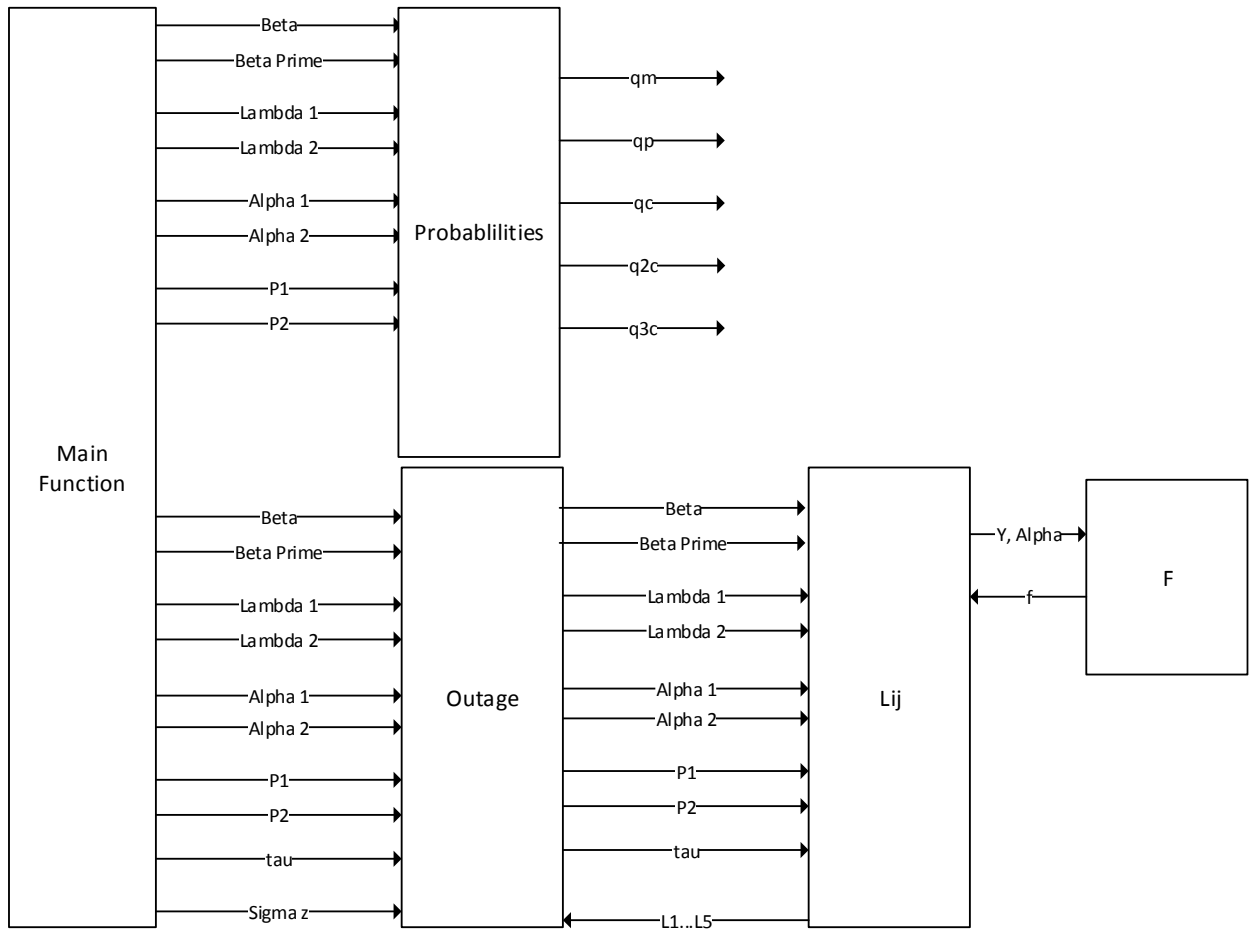
Figure 5: Summary of MATLAB analysis components

These input parameters call a function probabilities which evaluates the probability of having a UE in a particular mode of operation. Main also calls a function outage which calculates the outage probability with the help of the functions Lij (20-21) and F (22). The integral expressions were evaluated with the help of the MATLAB mathematics toolbox which contains the functions int, integral2, and integral3. The int function aids in evaluating simple single integrals, integral2 and integral3 evaluate double and triple integrals, respectively. The functions take as inputs the expression to be integrated along with the limits of integration.

5.2. Theoretical Analysis Replication on MATLAB

In order to obtain a fair comparison for our method, the results found in [13] were replicated. The parameters used were:

```
beta = 4;

lambda1 = 1/(500*500*pi);

lambda2 = 5*lambda1;

alpha1 = 4;

alpha2 = alpha1;

P1 = 37;
```

The results are shown in the figure below:
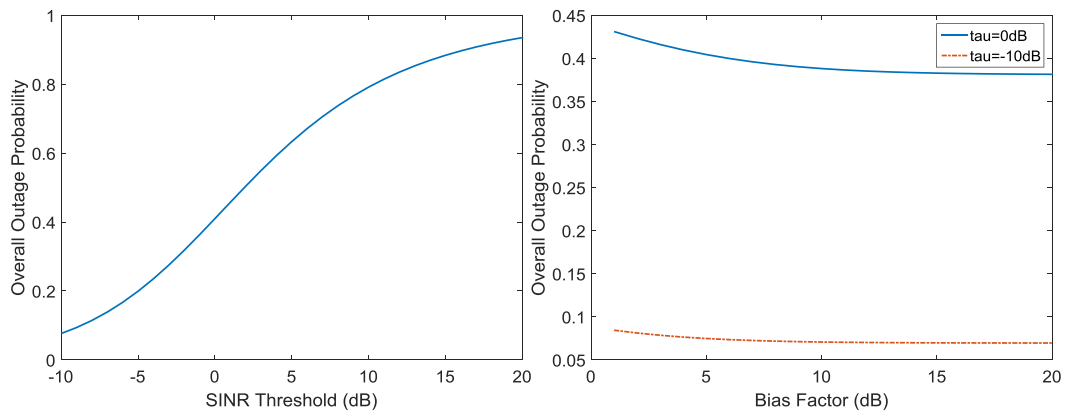
Figure 6: Overall Outage Probability vs SINR Threshold based on the parameters above (left). Overall Outage Probability vs Bias Factor based on the parameters above (right).

Fig.6 (left) shows the overall outage probability vs the SINR threshold in dB, while Fig.6 (right) shows the overall outage probability vs the bias factor in dB. It can be noted that these results are identical to those found in [15]. Furthermore, effect of varying tau can be explained the fact that for low values of the SINR threshold, we are being stricter and therefore can see more benefit to our scheme. These benefits begin to decrease as the SINR threshold is raised and no longer strict. As can be seen in Fig. 6 right, lowering the value of the SINR threshold results in the same trend in outage

probability, but shifted to lower values. In order to be consistent with the literature, we choose an SINR threshold of 0 dBs.

5.3. Simulation and Numerical Results

In this section, we simulate the effect of considering overlaps in microcell expanded regions on the overall performance of the network. Further analysis will also be provided to show the gains that are obtained for users that specifically lie within the microcell expanded region. These results are then compared with having no *3C* mode (systems in the literature), which means we only have cooperation between one macrocell and one microcell within the expanded region. This mode will be referred to as *2C* only.

The performed Monte Carlo simulation takes place within an area of 100 Km^2, where the transmission powers of the macro BS and micro BS are set to be 37dBm and 20dBm respectively. The variance for the AWGN channel is set to -104 dBm. Furthermore, the macrocell tier has a BS intensity of $(500^2\pi)^{-1}$ while the microcell tier BS intensity is 10 times that value. The BSs and UEs are simulated as independent Poisson Point Processes, and the analysis is done based on the resulting distance between the UEs and each BS. The intensity of UEs is set to be 20 times that of the macrocell tier. Finally, the pathloss exponents, α_1 and α_2, are set to 4.

In order to validate the experimental results, they are plotted against the theoretical ones based on the analysis discussed in the previous section. We compare the simulation results of varying the value of β from 0 to 20 to the results that are obtained

theoretically.

Figure 7: Outage probability vs β in a two tier cellular network with macrocell BS intensity is $(500^2\pi)^{-1}$ and microcells BS intensity $10(500^2\pi)^{-1}$. The SINR threshold is set to 0dB. Comparison to the results obtained from theoretical analysis is show.

As we can see in Fig.7 above, the theoretical results match with the experimental ones. All further results are based on experimental simulation.

Fig.8. demonstrates the fact that as the distance between the BSs increases, the outage probability increases as well. A lower average distance between the UE and base station indicates a lower micro BS intensity with respect to the macro BS. This is simulated by increasing the ratio of λ_1 to λ_2 from 1 (equal intensity) to 20. The UE intensity is fixed at twice the micro BS intensity.

Figure 8: Outage probability vs. average distance in a two tier cellular network with macrocell BS intensity is $(500^2\pi)^{-1}$ and microcells BS intensity varies from 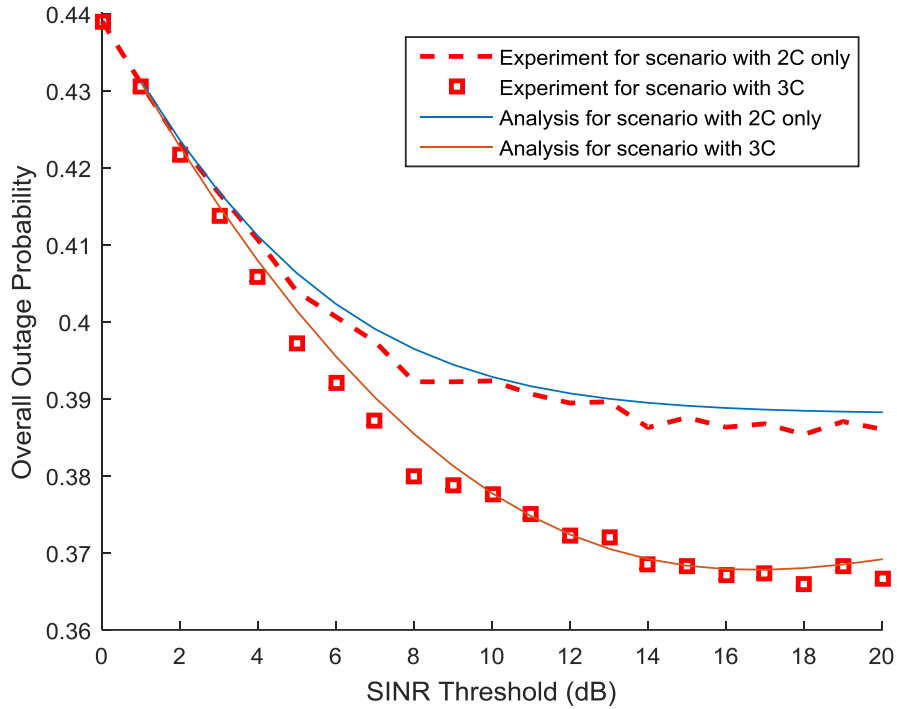$(500^2\pi)^{-1}$ to $20\ (500^2\pi)^{-1}$ (top left). Outage probability vs λ_2/λ_1 in a two tier cellular network with macrocell BS intensity is $(500^2\pi)^{-1}$ and microcells BS intensity varying from λ_1 to $20\ \lambda_1$. β and β' are set to 10dB (top right). The lower figures show the effect of having a microcell transmit power equal to 10 and 15 dBm respectively.

The results of the simulation indicate that as base station intensity increases, we can see more benefit in employing *3C* CoMP as the difference between the overall outage probabilities increases for lower average distance. This means that when base stations are located in close proximity, we can have more gains from the use of CoMP. Fig. 8 (left) further motivates the benefits of deploying *3C* comp in areas with densely populated BSs. Next, a series of experiments to further show the effect of *3C* on outage probability are discussed.

In order to further illustrate the benefit of considering overlapping ERs in densely crowded regions, we plotted the effect of varying relative BS intensities on the overall outage probability. The improvement in outage probability increases for more densely packed networks since the value of λ_2 indicates the number of microcells for each macrocell on average. As this ratio increases, the relative number of microcells with respect to macrocells rises and more overlap regions exist. This further motivates the benefits of deploying a CoMP scheme that takes into account overlaps in the microcell expanded regions. It can also be noted that the outage probability starts to increase after a certain point as the number of microcells increases in a fixed area. This can be explained by the fact that we are having an increase in the level of interference among microcells as they are operating at a relatively high power within such a small area. Decreasing the microcell BS transmit power would lead to a shift in the point at which outage probability start to increase, until we no longer have an increase in outage probability for lower transmit powers like at 10 dBm. This shows us that an unbounded increase in the microcell tier density would not be beneficial if the microcells are to continue to operate at the same power levels.

For the first experiment, the values of β and β' are set to 10dB, while the SINR threshold θ is varied between -10 and 20dB. The results can be seen in Fig. 10 (left) below, which indicates that the overall outage probability has decreased when overlaps in microcell ERs were considered. This shows that the proposed scheme results in superior performance in terms of outage probability. This is because we have considered, within the SINR expression, the effect of having another microcell nearby available for cooperation. This increases the value of the SINR at the concerned UEs

and lowers the overall outage probability, since we no longer have UEs susceptible to
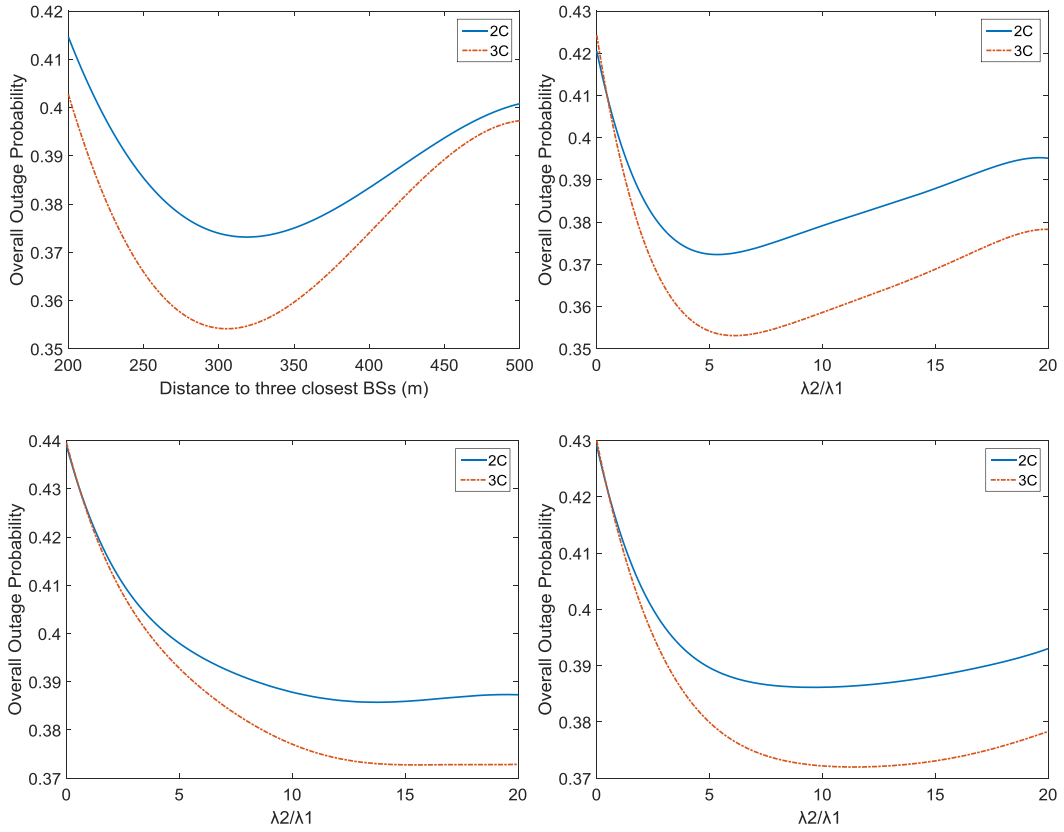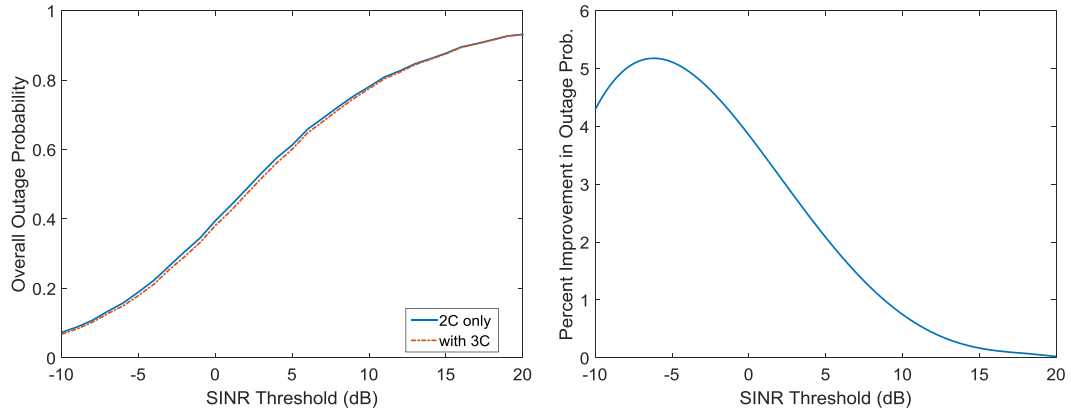
interference from nearby BSs.

Figure 9: Outage probability vs SINR threshold in a two tier cellular network with macrocell BS intensity is $(500^2\pi)^{-1}$ and microcells BS intensity $10(500^2\pi)^{-1}$. β and β' are set to 10dB (left). Percent Improvement in Outage probability vs SINR threshold in a two tier cellular network with macrocell BS intensity is $(500^2\pi)^{-1}$ and microcells BS intensity $10(500^2\pi)^{-1}$. β and β' are set to 10dB (right).

Fig. 9 (left) further elaborates on the overall gains that are obtained by

considering a CoMP scheme that takes into account the effect of microcell expanded

regions. It details the percent gain in overall outage probability for an expanded region

fixed at 10dB and an SINR threshold that varies from the value of -10 to 20 dBs. The

plot shows improvement in performance up to 5.5%, which decays as the SINR

threshold increases and becomes less strict.

Next, the effect of varying β is studied and its effect on overall outage

probability is shown. In this scenario, the value of β varies, along with β', from 0 to 20.

The SINR threshold θ is fixed at 0dB. The overall outage probability for the two

different schemes is shown. The results are as seen in Fig. 10.

The results indicate that the overall outage probability has decreased with a much lower floor as β increases. This is because as β increases, more users will be in the microcell ER, specifically, in the overlap region, leading to a better overall performance. The reason is that more users in the overlap region are having an SINR lower than the 0dB threshold.
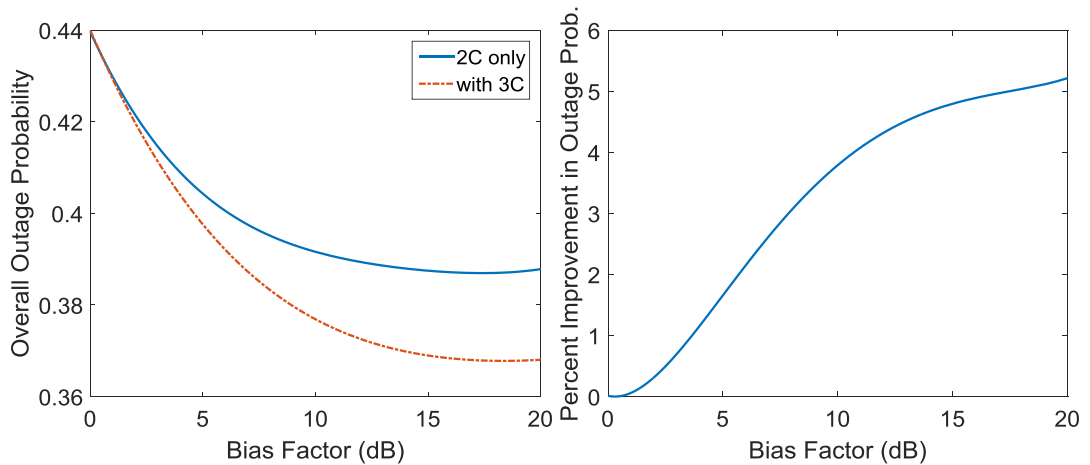
Figure 10: Outage probability vs β in a two tier cellular network with macrocell BS intensity is $(500^2\pi)^{-1}$ and microcells BS intensity $10(500^2\pi)^{-1}$. The SINR threshold is set to 0dB (left). Percent Improvement in Outage probability vs β in a two tier cellular network with macrocell BS intensity is $(500^2\pi)^{-1}$ and microcell BS intensity $10(500^2\pi)^{-1}$. The SINR threshold is set to 0dB (right).

Fig. 10 also illustrates the percentage improvement increases as the bias factor increases. This is because for higher bias factors, more users lie within the expanded regions and therefore more users can achieve better overall performance. This increase can be noted to be up to 5%, indicating that 5 of every 100 general users would have an SINR threshold that is higher than 0dB.

Finally, Fig. 11 shows the same scenario, but specifically details the effect on the outage probability of users within the microcell ER. Therefore, we can see how

much of a performance improvement is obtained for those users that lie within the ER due to considering the effect of overlap.

Figure 11: Outage probability vs β within the expanded region of a two tier cellular network with macrocell BS intensity is $(500^2\pi)^{-1}$ and microcell BS intensity $10(500^2\pi)^{-1}$. The SINR threshold is set to 0dB (left). Percent improvement in outage probability vs β within the expanded reg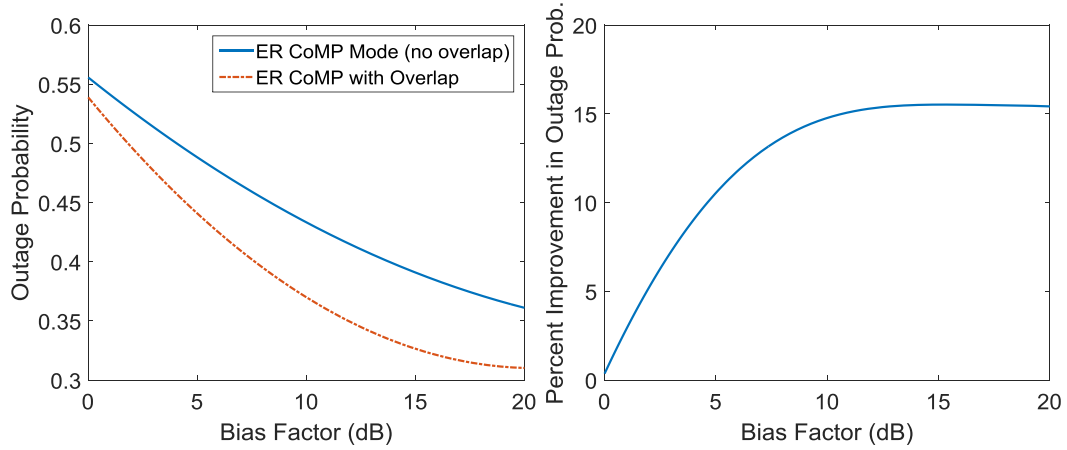ion of a two tier cellular network with macrocell BS intensity is $(500^2\pi)^{-1}$ and microcells BS intensity $10(500^2\pi)^{-1}$. The SINR threshold is set to 0dB (right).

As can be seen in Fig. 11, the outage probability decreases for users where we have cooperation among three base stations. Furthermore, the percentage improvement in outage probability for users within the overlap region can be seen on the right. The use of CoMP with three base stations within the overlap region brings significant performance improvement for users that lie within the ER. The increase in performance is up to 15%, which means that 15 out of a 100 users will experience an SINR level that is above 0 dB. For users that lie within this region, performance is seen to be significantly enhanced. This shows that the users who lie within these zones will have better performance and experience a lower outage probability due to the higher SINR obtained from increased cooperation. The simulation results indicate, that the proposed scheme brings improvement to the overall outage probability by improving network performance for UEs located within the microcell ERs.

51

CHAPTER VI

BACKHAUL CONSIDERATIONS

In order to begin studying the effect of having delay and capacity limitations on our system, some assumptions need to be outlined at first. In joint transmission coordinated multipoint (JT-CoMP), the macrocell base station receives the data packets intended to the UE of interest in the expanded region (ER) from the serving gateway (S-GW). Then, the macrocell BS designs the precoding vectors to be forwarded through a wired or wireless backhaul infrastructure to the other BSs in the cooperating cluster. Another option would be to send raw data along with the CSI and to allow the microcell BSs to perform the precoding. In wired environments, the types of delay that would be of greatest concern are transmission and propagation delay. On the other hand, in wireless we may have an additional access delay due to the possibility of having low SINR which forces retransmissions. There are two different wireless backhaul scenarios with either shared or dedicated resources. With shared resources, the backhaul network would be communicating using the same time and frequency resources as the UEs which increases interference. Dedicated resources mean that the backhaul transmissions are out of band, using millimeter wave frequencies for instance, and do not interfere with UE transmission and reception.

6.1. Effect on Backhaul Capacity

The use of Coordinated Multipoint Joint Transmission (JT-CoMP) leads to an increase in the amount of backhaul traffic. This is a direct result of the need for a serving base station to send user data to other BSs in the cooperating cluster for joint

transmission to the UE. To obtain an estimate of the capacity needed by a typical user, the spectral efficiency must be computed. Spectral efficiency is measured in bits/sec/Hz and indicates the data rate that can be provided over a given bandwidth. The spectral efficiency expression can be related to outage probability and is defined in (31) as in [15]:

$$SE_i = E_r \left[E_{SINR} \left[\log_2 (1 + SINR(B)) \right] \right] \tag{35}$$

$$SE_i = \int_A E_{SINR} \left[\log_2 (1 + SINR(B)) \right] f_{R_i}(r) dr \tag{36}$$

$$SE_i = \int_{R+} \left[\int_A P \left[\log_2 (1 + SINR(B)) > t \right] f_{R_i}(r) dr \right] dt \tag{37}$$

$$SE_i = \int_{R+} \left[\int_A P \left[SINR(B) > 2^t - 1 \right] f_{R_i}(r) dr \right] dt \tag{38}$$

From the definition of outage probability in (17) we can obtain the expression in (35):

$$SE_i = \int_{R+} 1 - \left[O_i \right]_{\tau = 2^t - 1} dt \tag{39}$$

Where B is the UE's mode of operation and i indexes the spectral efficiencies and distance probability density functions for the different modes of operation. Also, A is the area of integration based on user location in each mode of operation. O is the outage probability expression obtained in (19-22). Finally, the expression for overall spectral efficiency can be represented in (36) where q_M, q_P, q_{2C}, and q_{3C} are the probability of being in M, P, $2C$, and $3C$ respectively.

$$SE = q_M SE_M + q_P SE_p + q_{2C} SE_{2C} + q_{3C} SE_{3C} \tag{40}$$

53

Theoretical and experimental simulation results are analyzed based on different scenarios for spectral efficiency.

In the first scenario, analytical results are shown for varying the threshold for the microcell expanded region β from zero to 20 dB with CoMP in the microcell expanded region alone. The experimental results are plotted with the theoretical to demonstrate their validity.
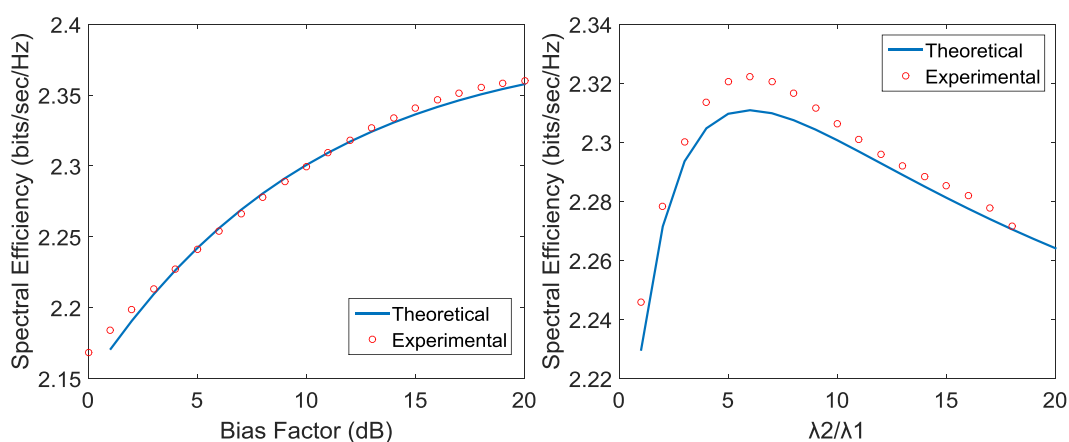

Figure 12: Overall spectral efficiency vs β within a two tier cellular network with macrocell BS intensity is $(500^2\pi)^{-1}$ and microcells BS intensity $10(500^2\pi)^{-1}$. The SINR threshold is set to 0dB (left). Overall spectral efficiency vs λ_2/λ_1 in a two tier cellular network with macrocell BS intensity is $(500^2\pi)^{-1}$ and microcells BS intensity varying from λ_1 to $20\,\lambda_1$. β and β' are set to 10dB (right). The mode of operation is 2C only.

As can be seen in Fig. 12 above, the overall spectral efficiency increases as the value of β increases. This can be explained by the fact that as the expanded region becomes larger, more UEs are being present in CoMP mode. This means that the SINR for these users has increased as a direct result of having their data transmitted from two BSs instead of one. At the same time, the experimental and analytical results overlap, which renders further validity to the analysis. In order to provide more insight and continue with our evaluation, the result of varying the microcell BS intensity is

presented on the right. As can be seen in fig.12 (right), the spectral efficiency keeps increasing where it peaks at a value about 6 for λ_2/λ_1. At this point, we have 6 times as many microcells as macrocells within our network. As the number of microcell BSs continues to rise, the spectral efficiency begins to drop due to the increase in interference from having multiple microcells operating within the transmission range of the macrocell. The results show the same trend theoretically and experimentally through simulations. This can be further explained by carefully looking into the regions that dictate a UE's mode of operation.
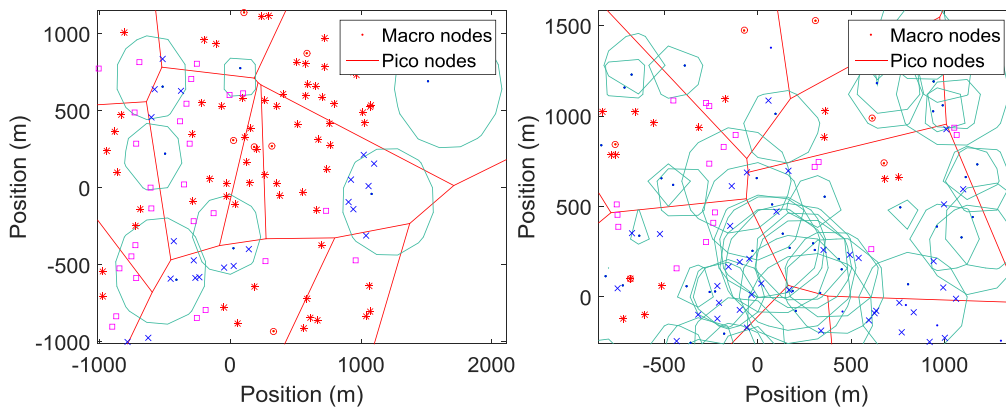

Figure 13: Base station and UE positions for two scenarios. Macrocell BS intensity is $(500^2\pi)^{-1}$ and microcells BS intensity is from λ_1 (left) and 8 λ_1 (right). β and β' are set to 10dB. Microcell BSs are represented as blue dots while macrocell BSs are represented as red circles with a dot in the center. Star shaped UEs are associated with the macrocell alone, x shaped UEs are associated with the microcell alone, and square UEs are in CoMP mode. The large circles represent the point where the power received from the macrocell becomes equal to the power received from the microcell.

Fig. 13 shows that as the number of microcell base stations increases, the overlaps between microcell BSs increases. As the number of microcells begins to rise within such a small area, we can see microcell BSs beginning to lie within the same

transmission range, which increases the amount of interference. This can be explained more intuitively by considering fig. 14 below.
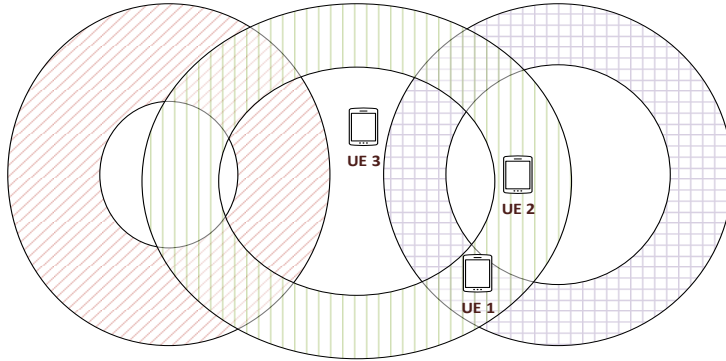

Figure 14: Representation of closely located microcells

Fig. 14 shows that as the number of microcells located close together becomes too high, there would be fewer UEs that may benefit from CoMP mode. This can be clarified by looking at UE 2 in fig. 20. UE 2 would be served by only one microcell BS since it lies within the region where the power received from the microcell is stronger than that of the macrocell. However, UE 2 would be suffering from an increase in the amount of interference due to having too many microcell BSs close to each other. On the other hand, UE 1 would be able to benefit from CoMP mode and UE 3 would receive a stronger signal from its serving BS. As we start to have more microcells close to each other, the number of UEs like UE 1 and UE 3's cases would start to decrease as interference continues to rise. This explains the intuition behind having an optimal value to the number of macrocell BSs with respect to a given number of macrocell BSs and an ER threshold β. The spectral efficiency values analyzed above will be used to calculate the percentage increase in the backhaul capacity due to having CoMP mode. In order to view the result of having CoMP on spectral efficiency in different scenarios, figure 15 is shown below:
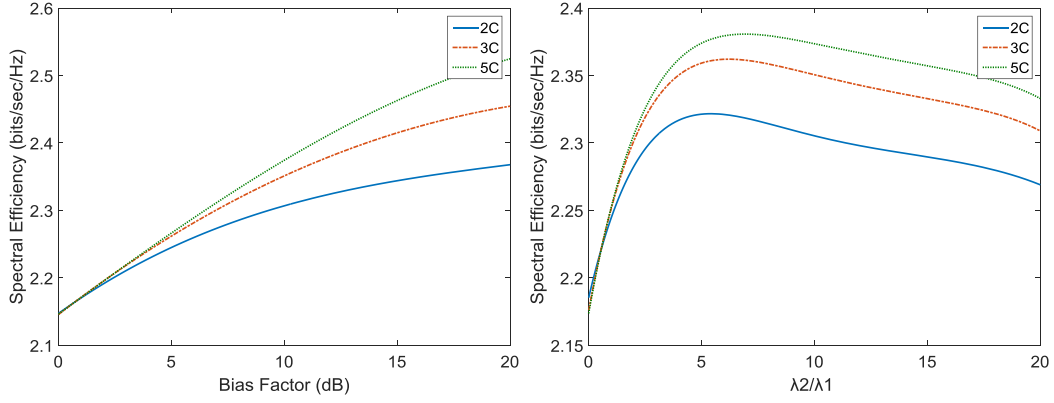
Figure 15: Overall Spectral efficiency vs β within a two tier cellular network with macrocell BS intensity is $(500^2\pi)^{-1}$ and microcells BS intensity $10(500^2\pi)^{-1}$. The SINR threshold is set to 0dB (left). Overall spectral efficiency vs λ_2/λ_1 in a two tier cellular network with macrocell BS intensity is $(500^2\pi)^{-1}$ and microcells BS intensity varying from λ_1 to $20 \lambda_1$. β and β' are set to 10dB (right).

The results in fig. 15 show that there is a direct relation between the spectral efficiency and the maximum number of BSs in the CoMP cluster. As the number of BSs in a cluster changes from 2 to 3 to 5, we can see that the spectral efficiency start to increase as a direct result of having more users in CoMP mode which leads to higher overall SINR.

As described in [31] the amount of X2 backhaul traffic connecting different BSs can be estimated as a percentage of S1 traffic which is the interface between the mobility management entity (MME) and the serving gateway (S-GW). According to [31], the amount of X2 traffic that accounts for handover is 4%, while the amount of traffic that takes into account transport protocol overhead is 10%. Based on these numbers and the analysis done in [27], we can state the amount of traffic passing through the backhaul is:

$$C = 1.14B(SE_i + SE_{CoMP})$$

(41)

$$SE_{CoMP} = \sum_{B \neq i} SE \qquad (42)$$

Where B is the bandwidth and SE_i is the spectral efficiency of each BS and

SE_{CoMP} is the spectral efficiency taking into account the data rates from other

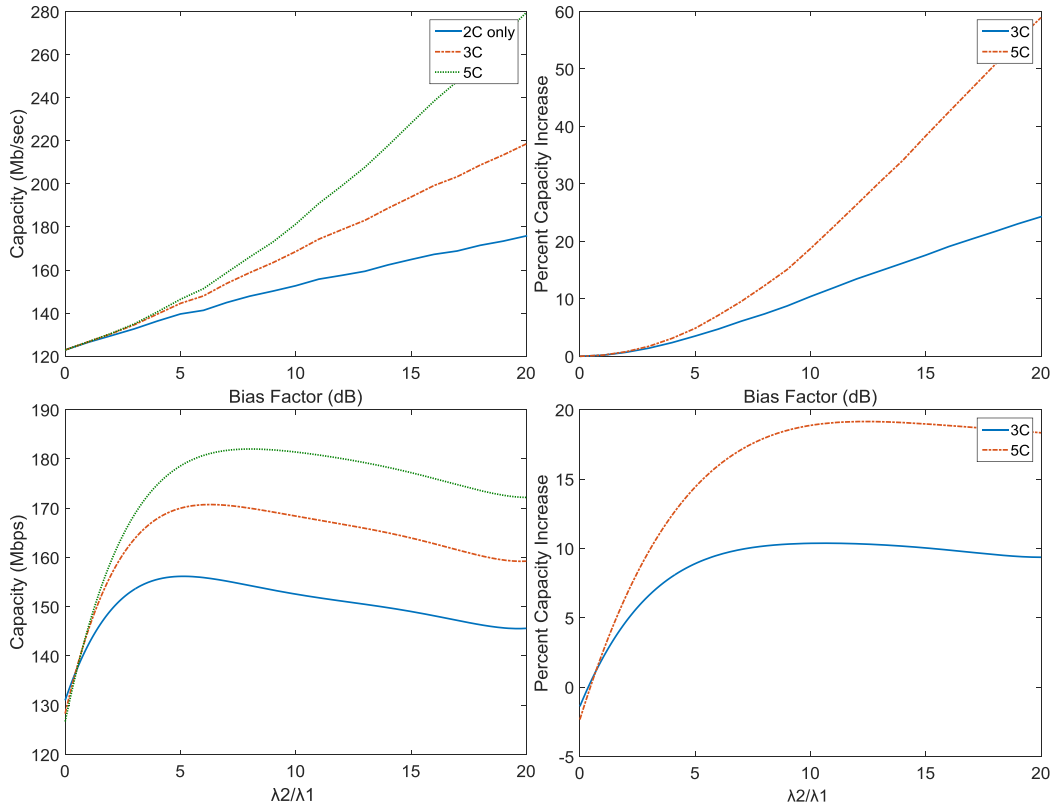cooperating BSs as seen in (38). Results as shown in fig. 16 below:

Figure 16: Capacity vs β within a two tier cellular network with macrocell BS intensity is $(500^2\pi)^{-1}$ and microcells BS intensity $10(500^2\pi)^{-1}$. The SINR threshold is set to 0dB (top). Capacity vs λ_2/λ_1 in a two tier cellular network with macrocell BS intensity is $(500^2\pi)^{-1}$ and microcells BS intensity varying from λ_1 to 20 λ_1. β and β' are set to 10dB (bottom). The rightmost figures show the percent increase in capacity.

The results shown in fig.15 indicate the capacity needed for backhaul network

provisioning. The results are shown for 3C mode as well as 5C mode. In 5C mode, four

macrocells, along with one microcell, cooperate in transmitting the same data to a UE.

As the number of BSs participating in CoMP increases, the overall traffic travelling on

the backhaul will increase. This is a direct result of the fact that the serving BS has to send user data to all other BSs participating in CoMP. Therefore, as the number of BSs in the CoMP group increases, the amount of backhaul traffic will rise by that amount. Furthermore, as the value of β increases, we have more users participating in CoMP mode, we can see the amount of backhaul traffic increasing up to 25% for 3C mode and up to 50% for 5C. On the other hand, as the number of microcells increase and for a fixed value of β, we can see that the backhaul traffic only increases up to a certain point, at 10% for 3C and 19% for 5C. This can be explained by the analysis done earlier. Since the increase in the amount of microcell BSs beyond a certain point causes significant interference, the overall SINR in the network decreases and this would lower the achievable rate.

6.2 Effect on Backhaul Delay

For the study of the impact of delay on our proposed system, we use the same infrastructure as described previously. The most significant types of delay to be discussed in relation to our system are the delays in wireless access and delays in the wired or wireless backhaul itself [22].

Let us first consider the effect of wireless delay. As discussed in [22], the wireless access delay is due to retransmissions from failed data packets. Retransmissions are allowed to occur up to M times, after that we have a failed transmission. A packet needs to be retransmitted whenever the SINR at a UE is below a certain threshold. This means that we can use the outage probability equations (18-21) to obtain the average overall wireless access delay. If T1 is the time taken for a single transmission from the BS to the UE, then the expected delay is greater than or equal to

T1 with probability 1, the probability of failure to occur one time is the outage probability itself which results in a delay of twice T1. The probability of a third failure is the outage probability squared and requires an added delay of T1 as well [22]. Therefore, the expected delay is:

$$E[D] = T_1[1 + O + O^2 + ... + O^{M-1}]$$

(43)

$$E[D] = \frac{T_1(1 - O^M)}{(1 - O)}$$

(44)

In Fig. 17, numerical results are provided for the average delay due to outage probability. The value of T1 was set to 1 and the simulation was run over values of microcell base station intensity varying from $(500 2\pi)^{-1}$ to 20 $(500 2\pi)^{-1}$. The macrocell base station intensity was fixed at $(500 2\pi)^{-1}$. At the same time, results are shown for fixing the microcell BS intensity at 10 $(500 2\pi)^{-1}$ and varying the expanded region threshold β from 0 to 20 dBs.

Figure 17: Overall delay vs β within a two tier cellular network with macrocell BS intensity is $(500^2 \pi)^{-1}$ and microcells BS intensity $10(500^2 \pi)^{-1}$. 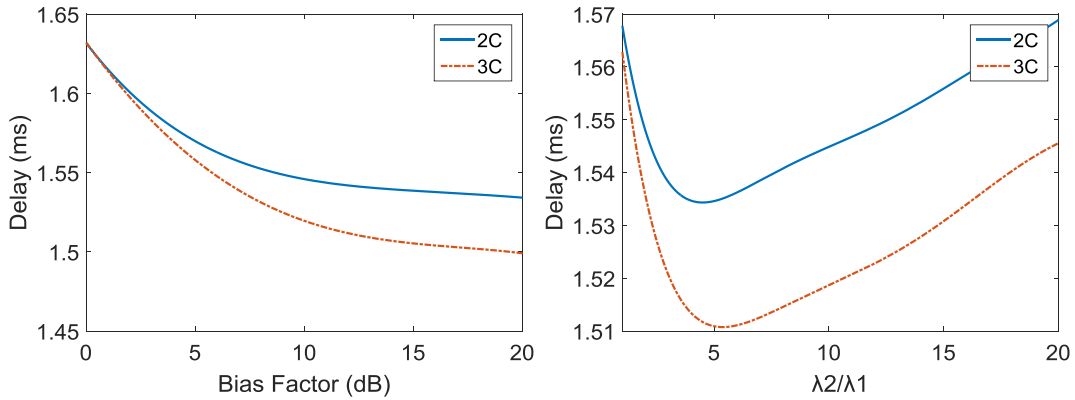The SINR threshold is set to 0dB (left). Overall delay vs λ_2/λ_1 in a two tier cellular network with macrocell BS intensity is $(500^2 \pi)^{-1}$ and microcells BS intensity varying from λ_1 to 20 λ_1. β and β' are set to 10dB (right).

As can be seen in figure 17 above, the delay due to wireless retransmissions from the BSs to the UEs depends on both β and the number of macrocell BSs in the network. As the value of β increases, the outage probability decreases and so does the overall number of retransmissions. However, when the number of microcell BSs continues to rise, we only have benefits up to a certain point, which is around 5 microcells to every macrocell. Further increasing the number of microcell BSs would lead to higher delay values.

Next, the effect of adding backhaul delay to the access delay obtained above is studied. The backhaul delay depends on the nature of the technology used. In this work, we will consider wired backhaul delay, wireless backhaul delay with dedicated resources and wireless backhaul delay with shared resources.

The wired backhaul can be modelled as a queue [32] and the delay can be obtained using Littles Law:

$$D = \frac{\lambda_{traffic}}{2\mu_{cap}\left(\mu_{cap} - \lambda_{traffic}\right)} \tag{45}$$

Where $\lambda_{traffic}$ is the amount of traffic on the backhaul links, and μ_{cap} is the backhaul link capacity. The delay value depends on the link capacity which we vary based on the results obtained in the surface plot shown in fig. 18 below. As can be seen, we have the highest spectral efficiency when β is 20 dB and λ_2 is at $6\lambda_1$. This can be explained as having lower overall SINR as β increases due to having more UEs in CoMP mode. At the same time, we can see that we have an optimal value at the peak of the surface plot for the number of microcell BSs. This means that beyond a certain value, the increase in the microcell BS intensity leads to a rise in the amount of interference experienced by the UE.
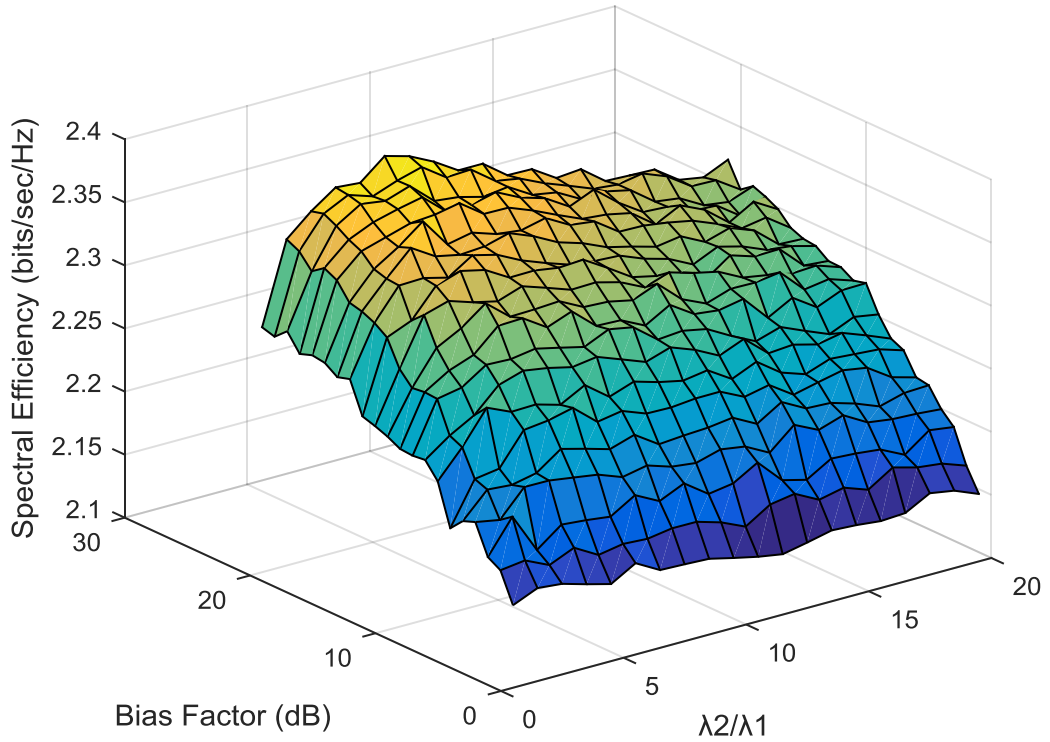
61

Figure 18: Overall delay vs β vs λ_2/λ_1 within a two tier cellular network with macrocell BS intensity is $(500^2\pi)^{-1}$ and microcells BS intensity varying from λ_1 to $20\,\lambda_1$. β and β' vary from 0 to 20dB.

Based on the results in fig. 18, we choose to consider a value of β equal to 20 dB and a value of λ_2 equal to $6\,\lambda_1$. At this point, the traffic travelling on the backhaul links is 132 Mbps. In order to have a stable system according to (41), the backhaul link capacity must be greater than the amount of traffic on the backhaul. Therefore, the capacity of the backhaul links in varied from 132 to 300 and the resulting delay can be seen in fig. 19.
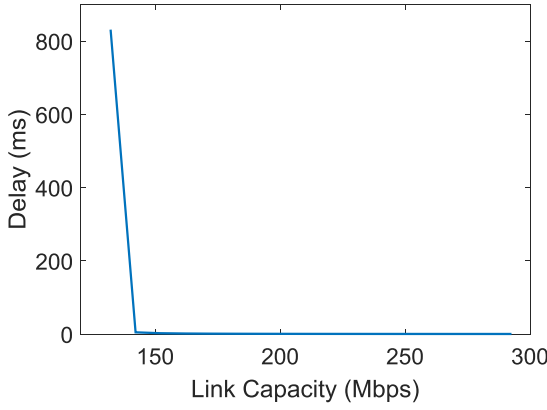
Figure 19: Link capacity (Mbps) vs Delay (ms) λ_1 within a two tier cellular network with macrocell BS intensity is $(500^2\pi)^{-1}$ and microcells BS intensity varying 6 λ_1. β and β' are set to 20dB.

Next, backhaul delay must be studied in terms of wireless links with shared resources. The wireless communication resulting from the X2 interface would interfere with other network transmissions. The microcell can be considered to have the same outage probability as a UE that associated with its macrocell with probability 1. That way, we can set q_M=1 and q_C=q_P=0.

$$f_{R_{bshared}}(r) = 2\pi\lambda_1 r \exp[-\pi(\lambda_1 r^2 + \lambda_2\left(\frac{\beta P_2}{P_1}\right)^{2/\alpha_2} r^{2\alpha_1/\alpha_2})] \tag{46}$$

In this case, it must be also be noted that the microcell BS is always receiving user data from the macrocell BS and therefore, the resulting outage probability would be similar to the one experienced by UEs connecting to the macrocell BS.

$$O_{backhaulshared} = 1 - \int_{R+} \exp\left[\frac{-\theta\sigma_z^2}{P_1 r^{-\alpha_1}}\right] \prod_{j=1}^{2} L_{I_j}\left(\frac{\theta r^{\alpha_1}}{P_1}\right) f_{R_{shared}}(r) dr \tag{47}$$

Finally, the outage probability in case we have dedicated resources can be treated as in [22], where the wireless backhaul is assumed not to interfere with the transmissions intended for UEs. In this case, we need to consider the probability density

63

function of the distance between two successive tiers in a Poisson Point Process. This is

shown in (44):

$$f_{R\,dedicated}(r) = 2\pi\lambda_1 r \exp[-\pi\lambda_1 r^2]$$

(48)

$$O_{backhaul,dedicated} = 1 - \int_{R+} \exp\left[\frac{-\theta\sigma_z^{\,2}}{P_1 r^{-\alpha_1}}\right] \prod_{j=1}^{2} L_{I_j}\left(\frac{\theta r^{\alpha_1}}{P_1}\right) f_{R_{dicated}}(r)dr$$

(49)

Finally, figure 20 shows the results of having all the different backhaul
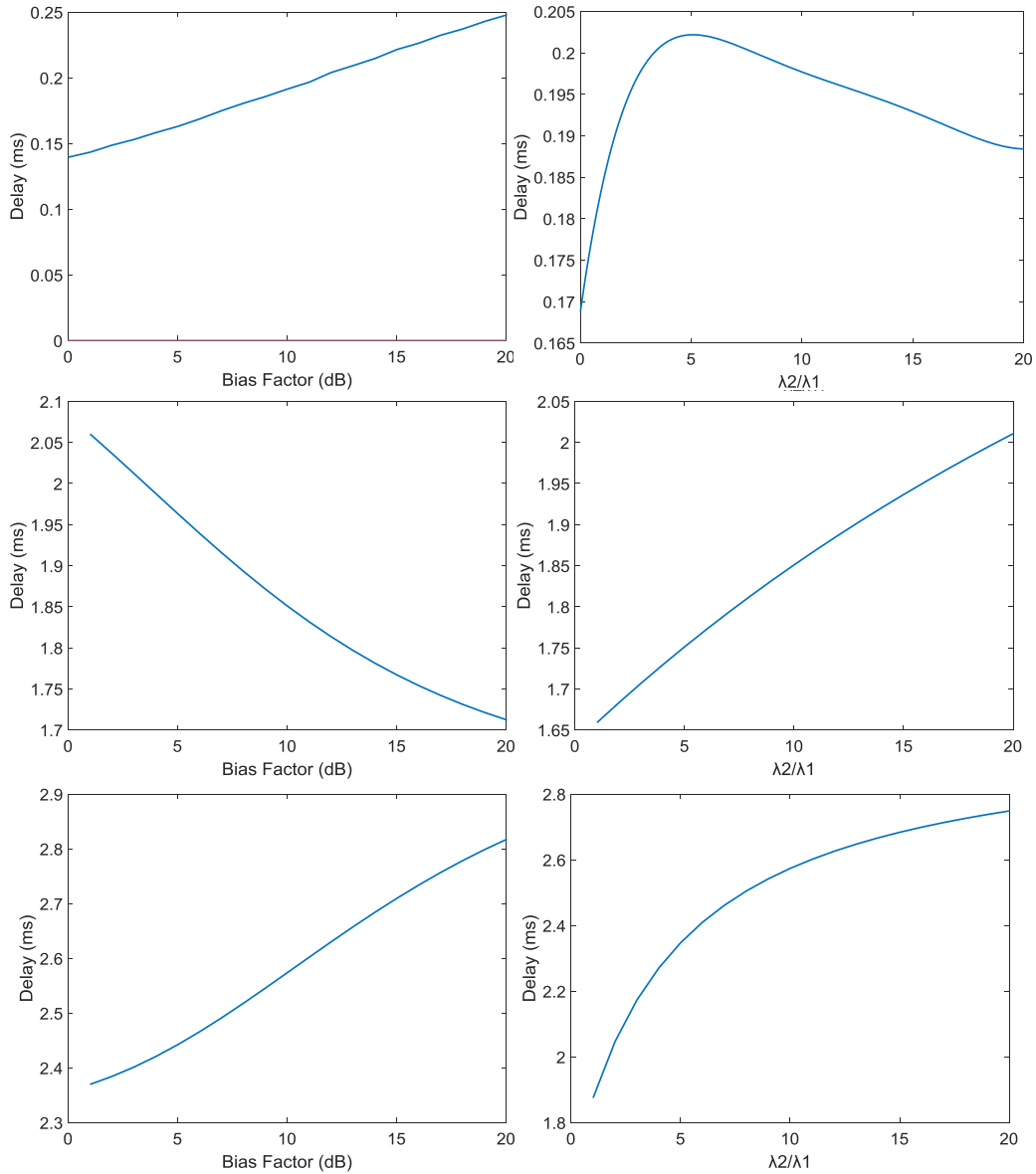
technologies:

64

Figure 20: Overall delay vs β within a two tier cellular network with macrocell BS intensity is $(500^2\pi)^{-1}$ and microcells BS intensity $10(500^2\pi)^{-1}$ (left). The SINR threshold is set to 0dB. Overall delay vs λ_2/λ_1 in a two tier cellular network with macrocell BS intensity is $(500^2\pi)^{-1}$ and microcells BS intensity varying from λ_1 to $20\lambda_1$. β and β' are set to 10dB (right). The topmost figures show delay for wired backhaul with 280 Mbps capacity. The middle figures show delay for wireless backhaul with dedicated resources. The bottom figures show delay for wireless backhaul with shared resources.

As can be seen in fig. 20 above, the backhaul delay relies on the technology used. For instance, wireless backhaul delay tells us that there is an optimal value for the microcell base station intensity beyond which performance begins to degrade. At the same time, we can see that the delay for wired backhaul starts to decrease beyond $6\lambda_2/\lambda_1$. This means that we can increase the number of microcell BSs at the expense of having lower overall SINR. Furthermore, as the bias factor increases, we can see a rise in delay as well except in the case of wireless delay with dedicated resources. This can be explained by the fact that as the bias factor start to increase, we would have more microcell BSs cooperating with the macrocell. This means that transmissions from macrocells to nearby microcells would no longer interfere with each other. At the same time, the signals transmitted from the macrocell to the microcell are not interfering with regular network traffic so we can benefit more from the reduced interference due to CoMP.

BIBLIOGRAPHY

[1]   I. F. Akyildiz, D. Gutierrez-Estevez, and E. Chavarria Reyes, "The Evolution to 4G Cellular Systems: LTE-Advanced," Physical Communications (Elsevier) Journal, vol. 3, no. 4, pp. 217–244, Dec. 2010.

[2]   I.F. Akyildiz, D.M. Gutierrez-Estevez, R. Balakrishnan, E. Chavarria Reyes, "LTE-Advanced and the Evolution to Beyond 4G (B4G) Systems," in Physical Communications (Elsevier) Journal, av. online, Nov. 2013.

[3]   D. Astely et al.; A Future-Radio-Access Framework; Journal on Selected Areas in Communications, Special Issue on 4G Wireless Systems.

[4]   Zirwas, Wolfgang; Zeeshan, Umer; Grieger, Michael, "Cooperative feeder links for relay enhanced networks," European Wireless, 2012. EW. 18th European Wireless Conference , vol., no., pp.1,8, 18-20 April 2012

[5]   ArrayComm. Cooper's Law. [Online]. Available: http://www.arraycomm.com/technology /coopers-law/

[6]   A. Sang, X. Wang, M. Madihian, and R. D. Gitlin, "Coordinated Load Balancing, Handoff/Cell-site Selection, and Scheduling in Multi-cell Packet Data Systems," in Proc. annual international conference on Mobile Computing and Networking (MOBICOM), pp. 302–314, 2004.

[7]   Lopez-Perez, D.; Xiaoli Chu; Guvenc, I., "On the Expanded Region of Picocells in Heterogeneous Networks," Selected Topics in Signal Processing, IEEE Journal of , vol.6, no.3, pp.281,294, June 2012

[8]   Han-Shin Jo; Young Jin Sang; Ping Xia; Andrews, J.G., "Heterogeneous Cellular Networks with Flexible Cell Association: A Comprehensive Downlink SINR Analysis," *Wireless Communications, IEEE Transactions on* , vol.11, no.10, pp.3484,3495, October 2012

[9]   Kshatriya, S.N.S.; Kaimalettu, S.; Yerrapareddy, S.R.; Milleth, K.; Akhtar, N., "On interference management based on subframe blanking in Heterogeneous LTE networks," Communication Systems and Networks (COMSNETS), 2013 Fifth International Conference on , vol., no., pp.1,7, 7-10 Jan. 2013

[10] H. Dhillon, R. Ganti, F. Baccelli, and J. Andrews, "Modeling and Analysis of K-Tier Downlink Heterogeneous Cellular Networks," IEEE Journal on Selected Areas in Communications (JSAC), vol. 30, no. 3, pp. 550–560, 2012.

[11] Mukherjee, S., "Distribution of Downlink SINR in Heterogeneous Cellular Networks," IEEE Journal on Selected Areas in Communications, vol. 30, no. 3, pp. 575,585, April 2012.

[12] Vajapeyam, M.; Damnjanovic, A.; Montojo, J.; TingfangJi; Yongbin Wei; Malladi, D., "Downlink FTP Performance of Heterogeneous Networks for LTE-

Advanced," Communications Workshops (ICC), 2011 IEEE International Conference on , vol., no., pp.1,5, 5-9 June 2011

[13] Daewon Lee; HanbyulSeo; Clerckx, B.; Hardouin, E.; Mazzarese, D.; Nagata, S.; Sayana, K., "Coordinated multipoint transmission and reception in LTE-advanced: deployment scenarios and operational challenges," Communications Magazine, IEEE , vol.50, no.2, pp.148,155, February 2012

[14] Nigam, G.; Minero, P.; Haenggi, M., "Coordinated Multipoint Joint Transmission in Heterogeneous Networks," Communications, IEEE Transactions on , vol.62, no.11, pp.4134,4146, Nov. 2014

[15] Sakr, A.H.; Hossain, E., "Location-Aware Cross-Tier Coordinated Multipoint Transmission in Two-Tier Cellular Networks," Wireless Communications, IEEE Transactions on , vol.13, no.11, pp.6311,6325, Nov. 2014

[16] Key Features. [Online]. Available: http://www.mathworks.com/products/matlab/features.html

[17] Marsch, P.; Fettweis, G., "A Framework for Optimizing the Uplink Performance of Distributed Antenna Systems under a Constrained Backhaul," in Communications, 2007. ICC '07. IEEE International Conference on , vol., no., pp.975-979, 24-28 June 2007

[18] Marsch, P.; Fettweis, G., "A Decentralized Optimization Approach to Backhaul-Constrained Distributed Antenna Systems," in Mobile and Wireless Communications Summit, 2007. 16th IST , vol., no., pp.1-5, 1-5 July 2007

[19] Marsch, P.; Fettweis, G., "On Base Station Cooperation Schemes for Downlink Network MIMO under a Constrained Backhaul," in Global Telecommunications Conference, 2008. IEEE GLOBECOM 2008. IEEE , vol., no., pp.1-6, Nov. 30 2008-Dec. 4 2008

[20] Biermann, T.; Scalia, L.; Changsoon Choi; Kellerer, W.; Karl, H., "How backhaul networks influence the feasibility of coordinated multipoint in cellular networks [Accepted From Open Call]," in Communications Magazine, IEEE , vol.51, no.8, pp.168-176, August 2013

[21] Chen, D.C.; Quek, T.Q.S.; Kountouris, M., "Wireless Backhaul in Small Cell Networks: Modelling and Analysis," in Vehicular Technology Conference (VTC Spring), 2014 IEEE 79th , vol., no., pp.1-6, 18-21 May 2014

[22] Chen, D.C.; Quek, T.Q.S.; Kountouris, M., "Backhauling in Heterogeneous Cellular Networks: Modeling and Tradeoffs," in Wireless Communications, IEEE Transactions on , vol.14, no.6, pp.3194-3206, June 2015

[23] Martin-Vega, F.J.; Di Renzo, M.; Aguayo-Torres, M.C.; Gomez, G.; Duong, T.Q., "Stochastic geometry modeling and analysis of backhaul-constrained Hyper-Dense

Heterogeneous cellular networks," in Transparent Optical Networks (ICTON), 2015 17th International Conference on , vol., no., pp.1-4, 5-9 July 2015

[24] Gongzheng Zhang; Quek, T.Q.S.; Aiping Huang; Kountouris, M.; Hangguan Shan, "Backhaul-aware base station association in two-tier heterogeneous cellular networks," in Signal Processing Advances in Wireless Communications (SPAWC), 2015 IEEE 16th International Workshop on , vol., no., pp.390-394, June 28 2015-July 1 2015

[25] Boccardi, F.; Huang, H.; Alexiou, A., "Network MIMO with reduced backhaul requirements by MAC coordination," in Signals, Systems and Computers, 2008 42nd Asilomar Conference on , vol., no., pp.1125-1129, 26-29 Oct. 2008

[26] Jungnickel, V.; Jaeckel, S.; Borner, K.; Schlosser, M.; Thiele, L., "Estimating the mobile backhaul traffic in distributed coordinated multi-point systems," in Wireless Communications and Networking Conference (WCNC), 2012 IEEE , vol., no., pp.3763-3768, 1-4 April 2012

[27] Jungnickel, V.; Manolakis, K.; Jaeckel, S.; Lossow, M.; Farkas, P.; Schlosser, M.; Braun, V., "Backhaul requirements for inter-site cooperation in heterogeneous LTE-Advanced networks," in Communications Workshops (ICC), 2013 IEEE International Conference on , vol., no., pp.905-910, 9-13 June 2013

[28] Mayer, Z.; Jingya Li; Papadogiannis, A.; Svensson, T., "On the impact of backhaul channel reliability on cooperative wireless networks," in Communications (ICC), 2013 IEEE International Conference on , vol., no., pp.5284-5289, 9-13 June 2013

[29] Samardzija, D.; Huang, H., "Determining backhaul bandwidth requirements for network MIMO," in Signal Processing Conference, 2009 17th European , vol., no., pp.1494-1498, 24-28 Aug. 2009

[30] Suryaprakash, V.; Fettweis, G.P., "An analysis of backhaul costs of radio access networks using stochastic geometry," in Communications (ICC), 2014 IEEE International Conference on , vol., no., pp.1035-1041, 10-14 June 2014

[31] J. Robson, "Guidelines for LTE Backhaul Traffic Estimation," NGMN White Paper, pp. 1–18, Jul. 2011.

[32] F. Pantisano, M. Bennis, W. Saad, M. Debbah and M. Latva-aho, "On the impact of heterogeneous backhauls on coordinated multipoint transmission in femtocell networks," *2012 IEEE International Conference on Communications (ICC)*, Ottawa, ON, 2012, pp. 5064-5069.